Distribution Category:
LMFBR Reactor Core Systems
(UC-79e)

ANL-77-78

ARGONNE NATIONAL LABORATORY
9700 South Cass Avenue
Argonne, Illinois 60439

A GENERAL MODEL FOR TURBULENT MOMENTUM AND HEAT TRANSPORT IN LIQUID METALS

by

William T. Sha and Brian E. Launder*

Components Technology Division

March 1979

*Consultant; University of California, Davis

TABLE OF CONTENTS

TABLE OF CONTENTS

LIST OF FIGURES

LIST OF TABLES

NOMENCLATURE

a	Constant appearing in Eq. 35
a'	Empirical constant in Eq. 54
b_u	Characteristic width of velocity field in free shear flow (for plane jet, b_u = half-width; for mixing layer distance between locations where normalized velocity is 0.1 and 0.9)
b_T	Characteristic width of temperature field defined analogously to b_u
c_p	Specific heat at constant pressure
c_v	Specific heat at constant volume
c_s, c_1, c_2, etc.	Empirical coefficients appearing in turbulence model. A complete list of coefficients and their recommended values appears in Table I.
E^*	Constant in near-wall "universal" velocity profile
F_1	Function of Pe_t (see Eq. 35)
f_1	Wall-effect function
G	Generation rate of turbulence energy due to buoyant effects
G_{ij}	Kinematic production rate of $\overline{u_i u_j}$ by buoyant forces
$G_{j\gamma}$	Kinematic production rate of $\overline{u_j \gamma}$ by buoyant interactions
g	Scalar energy, $\overline{\gamma^2}/2$
g_i	Component of gravitational acceleration in direction x_i
H	Enthalpy of fluid per unit mass
h	Fluctuating component of enthalpy
I	Internal energy of fluid per unit mass
K	Mean kinetic energy
k	Turbulence kinetic energy, $\overline{u_i^2}/2$
k^*	Kinetic energy at edge of viscosity-dependent region
ℓ	Dissipation length scale ($\epsilon = k^{3/2}/\ell$)
ℓ_m	Mixing length
n_k	Unit vector normal to a rigid surface
P	Function of Prandtl number, characterizing extra resistance of viscous layer to heat transport compared with momentum transport
P	Mean static pressure (as far as Eq. 19 only)
P	Generation rate of turbulence energy due to mean velocity gradients (beyond Eq. 19)
$\hat{P}$	Instantaneous static pressure
Pe	Peclet number
Pe_t	Turbulent Peclet number
P_g	Generation rate of g by mean temperature gradients
P_{ij}	Kinematic production rate of $\overline{u_i u_j}$ by mean velocity gradients
$P_{j\gamma}$	Kinematic production rate of $\overline{u_j \gamma}$ by mean velocity gradients
p	Fluctuation in static pressure
$\dot{q}'''$	Heat-generation rate per unit volume
$\dot{q}''_w$	Local heat-transfer rate per unit area from wall
R	Ratio of time scales of turbulent temperature and velocity fields
R_t^*	Reynolds number of edge of viscosity-dependent region $y^* k^{*1/2}/\nu$
T	Time period used for averaging mean quantities
T_{ij}	Net transport rate (i.e., convection minus diffusion) of $\overline{u_i u_j}$
T_j	Net transport rate of $\overline{u_j \gamma}$
T_k	Net transport rate of k
t	Time
$\hat{U}_i$	Instantaneous velocity in direction x_i

NOMENCLATURE

NOMENCLATURE

U_i	Mean component of velocity in x_i direction
u_i	Fluctuating (or turbulent component of velocity in x_i direction
$\overline{u_iu_j}$	Kinematic Reynolds stress
$\overline{u_iu_ju_k}$	Triple velocity correlation representing the diffusion rate of Reynolds stress $\overline{u_iu_j}$ in x_k direction
$\overline{u_j\gamma}$	Turbulent flux of enthalpy (divided by ρc_p)
x	Streamwise direction
x_i	Cartesian-space coordinate (tensor suffix notation)
x_n	Distance from wall
y^*	Thickness of viscosity-affected region next to a wall
y_e	Height of control volume above wall
y_P	Height of node next to wall above the surface
$\hat{\Gamma}$	Instantaneous temperature
Γ	Mean temperature
γ	Fluctuating (turbulent) temperature
δ_{ij}	Kronecker delta
ϵ	Kinematic dissipation rate of turbulence energy
$\bar{\epsilon}$	Mean value of ϵ over cell adjacent to a wall
ϵ_g	Kinematic dissipation rate of scalar energy
$\epsilon_{j\gamma}$	Dissipation rate of $\overline{u_j\gamma}$
κ^*	Constant in near-wall universal velocity profile
λ	Thermal conductivity
μ	Molecular (dynamic) viscosity
μ_t	Turbulent viscosity
ν	Kinematic viscosity
ρ	Density
ρ'	Fluctuations in density about mean (included in buoyant terms only)
τ	Shear stress
ζ	General mean value of dependent variable
ξ	Instantaneous value of dependent variable
φ_{ij}	Pressure-strain correlation (general)
$\varphi_{ij,1}$	First part of φ_{ij} (associated with turbulence-velocity interactions)
$\varphi_{ij,2}$	Second part of φ_{ij} (associated with mean strain)
$\varphi_{ij,3}$	Third part of φ_{ij} (associated with buoyancy)
$\varphi_{j\gamma}$	Pressure-temperature-gradient correlation (general)
$\varphi_{j\gamma,1}$, $\varphi_{j\gamma,2}$, $\varphi_{j\gamma,3}$	Denote turbulence, mean-strain, and buoyant parts of $\varphi_{j\gamma}$, respectively

Superscripts

$'$	Denotes instantaneous (mean plus turbulent) value of quantity
$*$	Values at edge of viscosity-affected region

Subscripts

e	Value at edge of finite-difference control volume next to wall
NP	Value at second node removed from wall
0	Value on axis
P	Value at node next to wall
t	Turbulent value
w	Wall value
∞	Value outside boundary layer

A GENERAL MODEL FOR TURBULENT MOMENTUM AND HEAT TRANSPORT IN LIQUID METALS

by

William T. Sha and Brian E. Launder

ABSTRACT

This report develops a general single-point closure scheme for calculating the local levels of turbulent fluxes of momentum and heat in liquid-metal flows. Transport effects are accounted for by way of the three scalar quantities: turbulence kinetic energy, k; turbulence-energy dissipation rate, ε; and scalar energy (or half the mean temperature variance), g. Their values at any point in the flow are obtained from the solution of conservation equations of transport type for each of the three quantities. The turbulent momentum fluxes (Reynolds stresses) and heat-transport rates are then obtained from algebraic formulas containing the above scalar quantities and the mean velocity and temperature fields.

Various applications of the model are discussed; the proposed model has a wide range of applicability.

I. INTRODUCTION

A. Class of Flows under Study

Despite their high cost and the precautions needed to handle them safely, liquid metals represent an attractive choice of fluid for certain heat-exchange processes because of their very high thermal conductivities. Circumstances that tend to favor liquid metals over less exotic coolants are those in which high heat-flux densities occur, particularly where flow rates are limited.

Two features of liquid-metal flow make the problem of estimating heat-transfer rates in, say, a prototype design much more difficult than where the working fluid is air or water. The first is the relative absence of detailed experimental data, due in part to the high cost of fabricating suitable apparatus and partly to the experimental difficulties of obtaining accurate statistical temperature-fluctuation data. The second feature is that, though the flow will nearly always be turbulent at design conditions, turbulent Peclet numbers are usually insufficiently high for molecular transport of heat to be negligible.

This has far-reaching implications in developing a theoretical model for such flows, for it means that we cannot invoke the usual high-Peclet-number concept of the large-scale temperature fluctuations being independent of the molecular transport properties of the fluid.

The present report provides state-of-the-art recommendations for modeling momentum and heat transport in liquid metals in a form suitable for use in finite-difference schemes for solving the three-dimensional momentum- and heat-transport equations. To make numerical simulations of three-dimensional flows will generally press hard on the available computer storage. There is thus a strong incentive to keep the turbulence model as simple as possible. This desire, however, is directly opposed by the sheer complexity and diversity of the flow structures that may arise in three-dimensional flow; only a highly sophisticated treatment could hope to predict results with sufficient accuracy over a wide range of conditions. In fact, a compromise treatment has been evolved; certain scalar properties of turbulence are obtained from solutions of transport equations (necessitating storage of these quantities over the field) while the turbulent momentum and heat fluxes are obtained point-by-point from a set of nonlinear algebraic equations.

Section II of this report develops the proposed form of the model and details the experimental results from which the proposals spring. Boundary conditions, particularly the near-wall treatment, are discussed in Sec. III; Sec. IV examines in somewhat greater detail a selection of convective transport problems, which may be successfully predicted with the model.

Although the report has been written with liquid-metal flows especially in mind, nearly all of what follows is applicable to flows of other single-phase fluids as well.

B. Class of Turbulence Models Selected

At present and, it appears, for at least the next decade, practical methods of calculating the behavior of turbulent flow must be based on the averaged form of the Navier-Stokes equations proposed by Reynolds at the end of the 19th century. In this scheme, all statistically random fluctuations in flow variables are averaged out, producing a set of transport equations for the mean properties. Through the nonlinearity of the convective transport processes, however, time-averaged correlations between pairs of velocity fluctuations or between enthalpy and velocity fluctuations remain in the mean flow equations. These correlations, representing additional transport rates of momentum and heat associated with the inherent unsteadiness of turbulent flow appear as unknowns to the equation set, and a theory or "turbulence model" is needed for their determination.

The earliest recognizable turbulence model was the mixing-length hypothesis (mlh) proposed by Taylor (1915) but, nowadays, usually associated

with the work of Prandtl (1925). According to this scheme, the transport rates due to turbulent agitation are determinable by introducing an equivalent turbulent viscosity μ_t whose magnitude is obtained from

$$\mu_t = \rho \ell_m^2 \sqrt{\frac{\partial U_i}{\partial x_\ell}\left(\frac{\partial U_i}{\partial x_\ell} + \frac{\partial U_\ell}{\partial x_i}\right)}, \qquad (1)$$

where ρ is the fluid density, U's denote mean velocities, x's are Cartesian coordinates, and the usual convention is adopted, wherein repeated suffixes implies summation over the three Cartesian components. The distribution of mixing length ℓ_m must be prescribed; implicit in the use of Eq. 1 is the idea that ℓ_m is a well-behaved function and that a few simple rules will suffice for its prescription over a range of flows.

The satisfactoriness of the $m\ell h$ could not be seriously tested until the 1960's when numerical-solution schemes became widely available for solving the fluid-flow equations for arbitrary two-dimensional flows. From this period of testing it emerged that the $m\ell h$ achieved significant success in predicting boundary layers developing along walls, that it was less successful at calculating the behavior of free shear flows, and that it was totally inadequate for predicting flows with recirculation such as may occur in the flow downstream from a sudden enlargement in pipe diameter. More recent explorations of three-dimensional flows have exposed further shortcomings in the model.

The deficiencies of the $m\ell h$, which make it unsuitable for use in a general computational scheme, may be attributed to two distinct causes. First, it links the local turbulent transport rate to local properties of the mean flow field. (In practice, the turbulent field, though ultimately owing its source of sustenance to the mean flow, will respond at different rates to any external changes.) Second, although in simple strain fields the idea of an isotropic turbulent viscosity has proved adequate, this is by no means the case when fluid undergoes more complex distortions.

Various workers have attempted to remove the former defect by devising transport equations for turbulence quantities that would be solved simultaneously with those for the mean flow; by this means the need to use mean-flow time and length scales to approximate turbulence scales was removed. Here we may mention the early work of Prandtl and Wieghardt (1945) which provided a transport equation for the turbulence kinetic energy, k. The turbulent viscosity was then evaluated from

$$\mu_t = \rho \ell k^{1/2}, \qquad (2)$$

where ℓ is an algebraically prescribed length scale displaying a variation similar to the mixing length.

Although conceptually the Prandtl-Wieghardt (1945) model represented a major advance over the $m\ell h$, in practical terms it achieved rather little.

Its achievements in free shear flows were modest (see, for example, comparative predictions of 23 free shear flows in Launder et al., 1972), and in recirculating flows, it was not at all satisfactory due to the largely "unguessable" distribution of length scale that arises in such flows. What was needed was a transport equation for the length scale--or for some related quantity from which the ℓ distribution could be calculated. Kolmogorov (1942) had, in fact, proposed such a "two-equation" model somewhat before the Prandtl-Wieghardt (1945) one-equation model. Kolmogorov's equation could not be tested for a further 25 years when computer programs had become available for obtaining numerical solutions of sequences of coupled, nonlinear partial differential equations. When it was tested, it was deficient in some respects.

Nevertheless, Kolmogorov's ideas stimulated the development of several other models in the late 1960's. Although these still fell somewhat short of providing universally valid models of turbulence, they at least provided a framework by means of which many turbulent recirculating flows have been successfully computed. The most widely used and probably the most successful of the two-equation models is that based on the transport equations for kinetic energy k and its dissipation rate ϵ. This model was evolved largely independently by workers at the Los Alamos Scientific Laboratories and the Imperial College, London [Daly and Harlow (1970); Hanjalić and Launder (1972); Jones and Launder (1972)].

The models mentioned so far all adopted the concept, due originally to St. Venant (though more usually attributed to Boussinesq), of an effective (isotropic) turbulent viscosity. There is no necessity to adopt this notion, however. As early as the mid 1940's, Chou (1945) had given the framework of an elaborate closure in which the Reynolds stresses (i.e., the correlations between two fluctuating velocities at a point) were themselves the subjects of a set of transport equations. In fact, Chou suggested that the triple velocity correlations, $\overline{u_i u_j u_k}$, would also be retained in transport form; thus, if his model were to be used for a general three-dimensional flow, 20 transport equations for turbulence quantities would need to be solved. Even with today's computers, this represents an impractically large number.

Some years later, Rotta (1951), taking a more down-to-earth approach, attempted to fill in the details around Chou's proposal and, at the same time, to cut the model down to manageable proportions. He made an algebraic rather than a differential approximation for the triple correlations, a level of modeling that has become known as a "second-order" or "Reynolds-stress" closure. Rotta's pioneering work in a sense appeared too early, for it was a further 15 years before the ideas he put forward could be tested, adapted, or borrowed by other workers in models of the same basic type.

There is an extensive literature, which we shall not attempt to cover in this short review. Mention is made, however, of the early contributions of Donaldson (1968) and Daly and Harlow (1970). Although their models did not

provide particularly good descriptions of turbulence, the appearance of these papers did a great deal to remove the hesitancy of solving so many strongly coupled transport equations. More recently, Launder, Reece, and Rodi (1975) published a model that has been applied by its originators to the prediction of a range of thin shear flows both close to and remote from walls.

What features make the differential Reynolds-stress model an attractive level of closure? There is not the fixed interrelationship between the local stresses and strain rate that the effective viscosity hypothesis enforces. In simple strain fields, where transport of the Reynolds stresses small, a Reynolds-stress model reduces to the effective viscosity hypothesis. But in flow over a curved surface, it leads to the prediction (in line with experiments) that the local shear stress is about 10 times as sensitive to the secondary strain associated with streamline curvature as to the primary strain. Likewise, for flow in a straight, noncircular duct, the model predicts that stresses in the plane of the duct cross section may be generated by strains in planes at right angles to these stresses. This characteristic, which is quite at odds with the concept of an effective viscosity, enables the phenomenon of turbulence-driven secondary flows to be correctly predicted.

A further advantage of a differential Reynolds-stress closure is that the influence of body forces on the turbulence structure appears quite naturally in the model without the need for ad hoc modifications. This is particularly important in buoyant flows, because the stratification affects both the turbulent stresses and the heat fluxes while the latter are coupled to the former through the gravitational term.

These considerations make it highly unlikely that one could devise generally adequate correlations of buoyant effects working within the framework of effective viscosity and (for heat transport) effective Prandtl number. With a second-order closure, however, the gross effects of buoyancy are well represented, even when rather primitive approximations are used for the unknown correlations [e.g., Donaldson, Sullivan, and Rosenbaum (1972); Mellor (1973)].

There is one respect, however, in which a second-order closure is not preferable to those based on the notion of an effective viscosity; this is the additional computer time required. With a differential stress model using a single length scale equation, seven transport equations must, in general, be solved for the hydrodynamic field and three more for the heat-flux correlations. The amount of computer core absorbed by holding the values of these correlations in store over the flow domain is sufficiently large to make one consider whether there are ways in which the benefits of the second-order closure can be retained while reducing the computing requirements to those akin to the two-equation effective viscosity models.

There has, in fact, emerged over the last few years a class of closure that can reasonably lay claim to possessing these dual qualities. Known as an

algebraic stress closure, it is arrived at by simplifying the transport stress in the Reynolds-stress transport equation so that the equation is reduced to algebraic form. Details of the simplification are presented in Sec. II.D. Application of this approach has been reported, inter alia, by Launder (1971) and Launder and Ying (1973) on the prediction of flow and heat transfer in square-sectioned ducts, Rodi (1972) on the normal-stress profiles in free jets, and Gibson and Launder (1976) on the prediction of horizontal free shear flows affected by buoyancy. A model of this kind is proposed for use in the present work.

The specific topic of heat transport in liquid metals has not previously received much attention within the framework of second-order transport models (or the simpler algebraic versions derived therefrom). The thesis of Owen (1973) appears to be the only work to have considered flows in which the Prandtl number was much less than unity. In fact, his modeling of the heat-flux equations was not particularly successful, the predicted distribution of turbulent Prandtl number showing (in contrast to experiments) an insignificant dependence on the Peclet number of the flow. Lawn (1977) made the interesting suggestion that the reduction of the heat fluxes at low Peclet number is due simply to the reduction of turbulent temperature fluctuations; that is, the correlation between velocity and temperature fluctuations is unaffected. There is not yet a sufficiently precise set of experimental data to allow the accuracy of this suggestion to be assessed. The current model, while permitting more subtle interactions than Lawn's suggestion allows, does take the view that the main effects of Peclet number arise from modifications to the time scale of the temperature-fluctuation field.

II. DEVELOPMENT OF MATHEMATICAL MODEL OF TURBULENCE

A. Mean Flow Equations

The Navier-Stokes equations governing the motion of a turbulent compressible fluid may be expressed, using Cartesian tensor notation, as

$$\rho\left(\frac{\partial \acute{U}_i}{\partial t} + \acute{U}_j\frac{\partial \acute{U}_i}{\partial x_j}\right) = -\frac{\partial \acute{P}}{\partial x_i} + \frac{\partial}{\partial x_j}(\acute{\tau}_{ji}) + \acute{\rho} g_i, \tag{3}$$

$$\frac{\partial \acute{\rho}}{\partial t} + \frac{\partial}{\partial x_i}(\rho \acute{U}_i) = 0, \tag{4}$$

and

$$\acute{\tau}_{ij} \quad \mu\left(\frac{\partial \acute{U}_i}{\partial x_j} + \frac{\partial \acute{U}_j}{\partial x_i}\right) - \frac{2}{3}\delta_{ij}\mu\frac{\partial \acute{U}_k}{\partial x_k}. \tag{5}$$

In the above equations, the $\acute{U}$'s indicate instantaneous values of velocity, $\acute{\rho}$ and $\acute{P}$ are the instantaneous density and static pressure, respectively, the x's are Cartesian space coordinates, g_i is the gravitational acceleration vector, and μ is the molecular viscosity. We note that the instantaneous density is retained only in the buoyant term of the momentum equation. Elsewhere, the "mean" density, ρ, defined below is used; the implications of this assumption are discussed shortly.

The time scale in which significant ordered variations of the flow take place is assumed to be more than an order of magnitude greater than the statistically random fluctuations associated with turbulence. We may thus distinguish mean and fluctuating flow components. Mean values of the dependent variables are defined as

$$\Phi(t) = \frac{1}{2T}\int_{-T}^{T} \hat{\Phi}\, dt, \tag{6}$$

where Φ stands for any of the dependent variables. The integration time T is chosen so that it is long compared with the turbulent time scales, but short compared with that needed for appreciable ordered variations to occur. We define φ, the turbulent component of Φ, as the difference between the instantaneous and mean values

$$\varphi \equiv \hat{\Phi} - \Phi. \tag{7}$$

Evidently, from Eq. 6,

$$\frac{1}{2T}\int_{-T}^{T} \varphi\, dt = 0; \tag{8}$$

i.e., the mean value of the fluctuating component is zero.

The decision to retain only the mean density on the left-hand sides of Eqs. 3 and 4 strictly implies that attention should be limited to situations in which the percentage fluctuations in density associated with turbulence are small compared with the percentage velocity fluctuations. The advantage of making this assumption is a great simplification in the task of characterizing the effects of turbulence in the later sections of this report. The assumption of negligible density fluctuations has commonly been made, even for calculating flows in which such an assumption is inapplicable; frequently (but not always), satisfactory predictions have been reported. {The interested reader may refer to the Proceedings of the Free Shear Flow Conference [NASA (1973)] in which more than a dozen computational schemes have been used to predict free shear flows involving substantial density gradients.}

Let us now replace the instantaneous properties in Eqs. 3 and 4 by the sum of the mean and fluctuating components, and then average the equations over the interval 2T. The equations for the transport of mean momentum may be written

$$\rho\left(\frac{\partial U_i}{\partial t} + U_j\frac{\partial U_i}{\partial x_j}\right) = -\frac{\partial P}{\partial x_i} + \frac{\partial \tau_{ji}}{\partial x_j} - \frac{\partial \rho\overline{u_i u_j}}{\partial x_j} + \rho g_i \tag{9}$$

and

$$\frac{\partial \rho}{\partial t} + \frac{\partial \rho U_i}{\partial x_j} = 0. \tag{10}$$

Equation 9, generally known as the Reynolds equation, provides the basis for all practical computations of turbulent flow. Due to the nonlinearity of the convective terms on the left of Eq. 3, the process of time averaging brings into prominence the correlation involving the turbulent velocities, $\rho\overline{u_i u_j}$. These correlations represent additional momentum fluxes or apparent stresses in the fluid (Reynolds stresses) over and above those associated with the mean motion. The magnitude of these correlations is unknown; thus the momentum and continuity equations no longer provide a closed set. Section II.C below develops a general theory for approximating these Reynolds stresses.

In analyzing heat transport by turbulence, we adopted an approach precisely analogous to that used above for the momentum equations. The first law of thermodynamics may be expressed in transport form as

$$\rho\left[\frac{\partial(\hat{I}+\hat{K})}{\partial t} + \hat{U}_j\frac{\partial(\hat{I}+\hat{K})}{\partial x_j}\right] = \frac{\partial}{\partial x_j}\left(\lambda\frac{\partial \hat{T}}{\partial x_j}\right) + \dot{q}''' - \frac{\partial \hat{P}\hat{U}_j}{\partial x_j} + \frac{\partial(\hat{\tau}_{ji}\hat{U}_i)}{\partial x_j} + \hat{\rho}\hat{U}_i g_i, \tag{11}$$

where $\hat{T}$, $\hat{I}$, and $\hat{K}$ denote the instantaneous values of temperature, internal energy, and kinetic energy of the fluid element, respectively, λ is its thermal

conductivity, and $\dot{q}'''$ represents the local heat generation rate per unit volume from sources other than the flow field (e.g., radiation or radioactive heat release). It is convenient to take the term containing static pressure to the left side of the equation. Then, on subtracting Eq. 3 multiplied by $\hat{U}_i$, we obtain

$$\frac{\partial}{\partial t}(\rho\hat{H}) + \frac{\partial}{\partial x_j}(\rho\hat{U}_j\hat{H}) = \frac{\partial}{\partial x_j}\left(\lambda\frac{\partial\hat{T}}{\partial x_j}\right) + \dot{q}''' + \hat{\tau}_{ji}\frac{\partial\hat{U}_i}{\partial x_j} + \left(\frac{\partial\hat{P}}{\partial t} + \hat{U}_i\frac{\partial\hat{P}}{\partial x_i}\right). \qquad (12)$$

As a result of this manipulation, the direct appearance of the reversible work terms and the kinetic energy has been eliminated through the introduction of the enthalpy $\hat{H}$, defined as $(\hat{I} + \hat{P}/\rho)$.

On expressing the instantaneous values of temperature, velocity, enthalpy, and pressure in terms of mean and fluctuating components and averaging the equation over an interval 2T, we obtain the mean enthalpy transport equation,

$$\rho\frac{\partial H}{\partial t} + \rho U_j\frac{\partial H}{\partial x_j} = \frac{\partial}{\partial x_j}\left(\lambda\frac{\partial T}{\partial x_j}\right) + \dot{q}''' + \tau_{ji}\frac{\partial U_i}{\partial x_j} + \rho\epsilon - \frac{\partial}{\partial x_j}(\rho\overline{u_j h})$$

$$+\left(\frac{\partial P}{\partial t} + U_i\frac{\partial P}{\partial x_i}\right) + \overline{u_i\frac{\partial p}{\partial x_i}}, \qquad (13)$$

where h denotes the instantaneous value of enthalpy fluctuation, ϵ is the mean value of the turbulence-kinetic-energy dissipation rate per unit mass, and the overbars imply, as usual, an averaging over an interval 2T. The correlation $u_i\,\partial p/\partial x_i$ principally represents a diffusive transport of turbulence energy by pressure fluctuations. Its influence, even in the turbulence-energy balance, is commonly negligible; therefore its retention in the mean enthalpy equation is unwarranted.

Alternatively, by way of the definition of the specific heat at constant pressure,

$$c_p = \left.\frac{\partial H}{\partial T}\right|_P,$$

we may, by assuming that the enthalpy is a function of temperature alone, reexpress Eq. 13 in the form

$$\rho c_p\left(\frac{\partial T}{\partial t} + U_j\frac{\partial T}{\partial x_j}\right) = \frac{\partial}{\partial x_j}\left(\lambda\frac{\partial T}{\partial x_j}\right) + \dot{q}''' - \frac{\partial}{\partial x_j}(\rho c_p\overline{u_j T}) + \tau_{ji}\frac{\partial U_i}{\partial x_j}$$

$$+ \rho\epsilon + \left(\frac{\partial P}{\partial t} + U_i\frac{\partial P}{\partial x_i}\right). \qquad (14)$$

The correlation $\overline{u_j\gamma}$ on the right side of Eq. 14 is, like the Reynolds stresses in the mean momentum equation, an unknown to our system of equations; it is proportional to the extra rate of enthalpy transport due to the turbulent fluctuations. Section II.C below presents proposals for modeling this quantity; first, however, we will develop an exact equation describing the transport of $\overline{u_j\gamma}$.

The turbulence-energy dissipation rate is also an unknown quantity for whose determination a scheme is proposed in Sec. III.

B. Exact Transport Equations Governing the Level of $\overline{u_iu_j}$ and $\overline{u_j\gamma}$

We note first that, on subtracting Eq. 10 from Eq. 4, we obtain the continuity equation governing the turbulent motion:

$$\frac{\partial}{\partial x_j}(\rho u_j) = 0. \tag{15}$$

Moreover, subtraction of Eq. 9 from Eq. 3 produces, with the help of Eq. 15, the following transport equation governing the level of fluctuating velocity u_i:

$$\rho\left(\frac{\partial u_i}{\partial t} + U_k\frac{\partial u_i}{\partial x_k}\right) = -\frac{\partial p}{\partial x_i} - \rho u_k\frac{\partial U_i}{\partial x_k} - \frac{\partial}{\partial x_k}(\rho u_iu_k - \rho\overline{u_iu_k})$$

$$+ \frac{\partial}{\partial x_k}\left[\mu\left(\frac{\partial u_i}{\partial x_k} + \frac{\partial u_k}{\partial x_i}\right)\right] + \rho' g_i, \tag{16}$$

where ρ' denotes the turbulent density fluctuation and, for reasons that will become apparent below, the subscript j has been replaced by k. (This replacement has no effect on the equation, since the subscript appears twice in each term and summation for the three Cartesian directions is thus indicated.) In Eq. 16, the compressible part of Stokes' stress-strain law has been neglected.

Now let us multiply Eq. 15 by u_j and add it to its complementary equation in which subscripts i and j have been interchanged. On time-averaging and regrouping, we now have an equation for the transport of the correlation $\overline{u_iu_j}$:

$$\rho\left(\frac{\partial\overline{u_iu_j}}{\partial t} + U_k\frac{\partial\overline{u_iu_j}}{\partial x_k}\right) = \underbrace{-\rho\left(\overline{u_iu_k}\frac{\partial U_j}{\partial x_k} + \overline{u_ju_k}\frac{\partial U_i}{\partial x_k}\right)}_{A} + \underbrace{(\overline{\rho' u_i}g_j + \overline{\rho' u_j}g_i)}_{B} - \underbrace{\left[\overline{\mu\frac{\partial u_j}{\partial x_k}\left(\frac{\partial u_i}{\partial x_k} + \frac{\partial u_k}{\partial x_i}\right)} + \overline{\mu\frac{\partial u_i}{\partial x_k}\left(\frac{\partial u_j}{\partial x_k} + \frac{\partial u_k}{\partial x_j}\right)}\right]}_{C}$$

$$+ \underbrace{\overline{p\left(\frac{\partial u_i}{\partial x_j} + \frac{\partial u_j}{\partial x_i}\right)}}_{D} + \underbrace{\frac{\partial}{\partial x_k}\left[\mu\left(\frac{\partial\overline{u_iu_j}}{\partial x_k} + \frac{\partial\overline{u_ku_j}}{\partial x_i} + \frac{\partial\overline{u_ku_i}}{\partial x_j}\right) - \rho\,\overline{u_iu_ju_k} - (\overline{pu_i}\delta_{jk} + \overline{pu_j}\delta_{ik})\right]}_{E}. \tag{17}$$

This equation expresses the fact that the total rate of increase of $\overline{u_i u_j}$ for an elemental fluid packet is equal to the excess of the generation rate due to mean shear (A) and buoyant interactions (B), over the loss through viscous dissipation (C), through the randomizing action of the pressure-strain correlation (D), and through diffusive transport (E). Section II.C considers the simplification and closure of this equation.

An equation for the transport of turbulent temperature fluctuations may be obtained by subtracting Eq. 14 from Eq. 12 (the latter having been expressed in terms of temperature rather than enthalpy). The resultant equation may be written

$$\rho c_p\left(\frac{\partial \gamma}{\partial t} + U_k\frac{\partial \gamma}{\partial x_k}\right) = -\rho c_p u_k\frac{\partial \Gamma}{\partial x_k} - c_p\frac{\partial}{\partial x_k}(\rho u_k\gamma - \rho\overline{u_k\gamma}) + \frac{\partial}{\partial x_k}\left(\lambda\frac{\partial \gamma}{\partial x_k}\right) + 2\mu\frac{\partial U_i}{\partial x_k}\left(\frac{\partial u_i}{\partial x_k} + \frac{\partial u_k}{\partial x_i}\right) + \left[\mu\frac{\partial u_i}{\partial x_k}\left(\frac{\partial u_i}{\partial x_k} + \frac{\partial u_k}{\partial x_i}\right) - \mu\overline{\frac{\partial u_i}{\partial x_k}\left(\frac{\partial u_i}{\partial x_k} + \frac{\partial u_k}{\partial x_i}\right)}\right] + \frac{\partial p}{\partial t} + u_k\frac{\partial P}{\partial x_k} + U_k\frac{\partial p}{\partial x_k} + \left(u_i\frac{\partial p}{\partial x_i} - \overline{u_i\frac{\partial p}{\partial x_i}}\right). \qquad (18)$$

On multiplying through by u_j and adding to the resultant equation that is obtained by multiplying Eq. 16 (with the subscript j replacing i) by $\overline{c_p\gamma}$, we produce an equation describing the transport of the correlation $\overline{u_j\gamma}$ along a streamline:

$$\rho\left(\frac{\partial}{\partial t}\overline{u_j\gamma} + U_k\frac{\partial \overline{u_j\gamma}}{\partial x_k}\right) = \underbrace{-\rho\overline{u_j u_k}\frac{\partial \Gamma}{\partial x_k}}_{A} \underbrace{-\rho\overline{u_k\gamma}\frac{\partial U_j}{\partial x_k}}_{B} + \underbrace{\overline{\rho'\gamma g_j}}_{C} \underbrace{-\left[\mu\overline{\frac{\partial \gamma}{\partial x_k}\left(\frac{\partial u_j}{\partial x_k} + \frac{\partial u_k}{\partial x_j}\right)} + \frac{\lambda}{c_p}\overline{\frac{\partial \gamma}{\partial x_k}\frac{\partial u_j}{\partial x_k}}\right]}_{D} + \underbrace{\overline{p\frac{\partial \gamma}{\partial x_j}}}_{E} - \underbrace{\frac{\partial}{\partial x_k}\left[\rho\overline{u_k u_j\gamma} + \overline{p\gamma}\,\delta_{jk} - \frac{\lambda}{c_p}\overline{u_j\frac{\partial \gamma}{\partial x_k}} - \mu\overline{\gamma\left(\frac{\partial u_j}{\partial x_k} + \frac{\partial u_k}{\partial x_j}\right)}\right]}_{F} + \underbrace{\overline{\rho u_j\frac{\partial \gamma}{\partial t}\left(1 - \frac{c_v}{c_p}\right)}}_{G} \qquad (19)\ \text{(Contd.)}$$

$$
\left.
\begin{aligned}
&\text{---------- (broken line) ----------} \\
&+ 2\frac{\mu}{c_p}\frac{\partial U_i}{\partial x_k}\overline{u_j\left(\frac{\partial u_i}{\partial x_k} + \frac{\partial u_k}{\partial x_i}\right)} \\
&+ \frac{\mu}{c_p}\overline{u_j\frac{\partial u_i}{\partial x_k}\left(\frac{\partial u_i}{\partial x_k} + \frac{\partial u_k}{\partial x_i}\right)} \\
&+ \overline{\frac{u_j}{c_p}\frac{\partial p}{\partial t}} + \overline{\frac{u_j u_k}{c_p}}\frac{\partial P}{\partial x_k} + \frac{U_k}{c_p}\overline{u_j\frac{\partial p}{\partial x_k}} + \overline{\frac{u_k u_j}{c_p}\frac{\partial p}{\partial x_k}}.
\end{aligned}
\right\} \text{(Contd.)} \quad (19)
$$

The processes on the right-hand side of Eq. 19 causing the correlation $\overline{u_j\gamma}$ to change along a streamline may be interpreted as generative agencies arising from mean temperature and velocity gradients (A and B) and gravitational action (C); molecular smearing in the fine-scale motion (D); destruction due to the randomizing action of the fluctuating pressure field (E); diffusive transport due to both molecular and turbulent mixing (F); and to an effect, in nonstationary gaseous flows, associated with the nonequality of the specific heats at constant pressure and constant volume (G). There are, in addition, the correlations appearing below the broken line arising from viscous heating and pressure gradients. Their influence will be insignificant unless the Eckert number is of order unity. These conditions will occur only when heat transport through the flow boundaries is small compared with that generated internally by friction or compression. Such a situation is so far removed from those encountered in the heat-exchanger area that the terms are hereafter discarded in the main text. The question of approximating the unknown correlations appearing above the broken line is discussed further in Secs. II.C.3-II.C.8.

Before leaving consideration of the exact equations, we shall obtain transport equations for the scalar quantities $k(\equiv \overline{u_i^2}/2)$ and $g(\equiv \overline{\gamma^2}/2)$. These are readily derived by multiplying Eq. 15 by u_i and Eq. 17 by γ. The resulting equations may be written

$$
\rho\left(\frac{\partial k}{\partial t} + U_k\frac{\partial k}{\partial x_k}\right) = \underbrace{-\rho\overline{u_i u_k}\frac{\partial U_i}{\partial x_k}}_{\rho P} + \underbrace{\overline{\rho' u_i} g_i}_{\rho G} \underbrace{- \mu\overline{\frac{\partial u_i}{\partial x_k}\left(\frac{\partial u_i}{\partial x_k} + \frac{\partial u_k}{\partial x_i}\right)}}_{\rho\epsilon}
$$

$$
+ \frac{\partial}{\partial x_k}\left[\mu\left(\frac{\partial k}{\partial x_k} + \overline{\frac{\partial u_i u_k}{\partial x_i}}\right) - \rho\overline{\frac{u_i^2 u_k}{2}} - \overline{p u_i}\delta_{ik}\right] \quad (20)
$$

and

$$
\rho\left(c_v\frac{\partial g}{\partial t} + c_p U_k\frac{\partial g}{\partial x_k}\right) = -\rho c_p\overline{u_k\gamma}\frac{\partial \Gamma}{\partial x_k} - \lambda\overline{\frac{\partial\gamma}{\partial x_k}\frac{\partial\gamma}{\partial x_k}} + \frac{\partial}{\partial x_k}\left(\lambda\frac{\partial g}{\partial x_k} - \rho\overline{\frac{u_k\gamma^2}{2}}\right). \quad (21)
$$

As remarked above, viscous and compressive terms are dropped from Eq. 21.

These equations are evidently simpler in character than the Reynolds-stress and velocity-temperature-correlation equations derived earlier. We shall take advantage of this simplicity in Sec. II.D.1 to devise a convenient, economical form of our model for practical computations.

C. Closure Proposals for $\overline{u_iu_j}$ and $\overline{u_j\gamma}$ Equations

1. The High-Reynolds-number Approximation

We shall assume that, except in the immediate vicinity of rigid boundaries (for which, in any event, special provision is made later), viscous transport effects are negligible in comparison with turbulent transport. This is equivalent to saying that the large-scale turbulent motions that carry the turbulent energy and Reynolds stress are unaffected by fine-scale motions. Reciprocally, the fine-scale motions, which are directly influenced by viscosity, are assumed to be unaware of the character of the large-scale turbulence or of the mean flow.

This assumption greatly simplifies the task of devising a closed form of Eq. 17. First, the viscous dissipation of $\overline{u_iu_j}$ can be represented in the form appropriate to isotropic turbulence:

$$\mu\left[\overline{\frac{\partial u_i}{\partial x_k}\left(\frac{\partial u_j}{\partial x_k}+\frac{\partial u_k}{\partial x_j}\right)}+\overline{\frac{\partial u_j}{\partial x_k}\left(\frac{\partial u_i}{\partial x_k}+\frac{\partial u_k}{\partial x_i}\right)}\right]=\tfrac{2}{3}\delta_{ij}\epsilon, \tag{22}$$

where ϵ is the dissipation rate of turbulence energy, which, at high Reynolds numbers reduces to

$$\epsilon=\mu\overline{\frac{\partial u_i}{\partial x_k}\frac{\partial u_i}{\partial x_k}}. \tag{23}$$

We may also neglect the viscous contributions to the diffusion term (E) in Eq. 17. Further, in seeking approximations for the remaining unknowns in this equation, we consider forms that are independent of viscosity.

2. Diffusive Transport of Stress

Hanjalić and Launder (1972) devised the following approximation for the triple-velocity correlation $\overline{u_iu_ju_k}$:

$$-\overline{u_iu_ju_k}=c_s'\frac{k}{\epsilon}\left(\overline{u_ku_\ell}\frac{\partial\overline{u_iu_j}}{\partial x_\ell}+\overline{u_ju_\ell}\frac{\partial\overline{u_ku_i}}{\partial x_\ell}+\overline{u_iu_\ell}\frac{\partial\overline{u_ju_k}}{\partial x_\ell}\right), \tag{24}$$

where the empirical coefficient c_s' was later optimized by Launder, Reece, and Rodi (1975) as 0.11. The latter work found, however, that the simpler form proposed by Daly and Harlow (1970) appeared to give just as satisfactory results:

$$-\overline{u_i u_j u_k} = c_s \frac{k}{\epsilon} \overline{u_k u_\ell} \frac{\partial \overline{u_i u_j}}{\partial x_\ell}, \tag{25}$$

where the coefficient c_s was taken as 0.22. In retrospect, although Eq. 24 is a better model of $\overline{u_i u_j u_k}$ than Eq. 25, it seems likely that the latter is equally good as a model of the total turbulent transport of $\overline{u_i u_j}$. (Launder, Reece, and Rodi had omitted any modeling of the pressure-transport term.)

3. Pressure-Strain Correlation

The pressure-strain correlation in Eq. 16 represents arguably the most crucial term to model in the Reynolds-stress equation. In fact, three distinct agencies contribute to the fluctuating pressure field, each of which will need separate modeling. This becomes apparent by taking the x_i derivative of the equation for the turbulent velocity fluctuation (Eq. 16). After rearrangement, we obtain

$$\frac{1}{\rho} \frac{\partial^2 p}{\partial x_i^2} = \underbrace{\frac{\partial^2}{\partial x_k \partial x_i} (u_i u_k - \overline{u_i u_k})}_{(A)} - \underbrace{2 \frac{\partial u_k}{\partial x_i} \frac{\partial U_i}{\partial x_k}}_{(B)} + \underbrace{g_i \frac{\partial \rho'}{\partial x_i}}_{(C)}. \tag{26}$$

From Eq. 26 it may be inferred that the pressure fluctuations are induced by purely turbulence interactions (A), effects involving the mean rate of strain (B), and buoyant contributions (C). Although some workers still include an approximation of only the first of these contributions, there is a gradually emerging awareness of the important contribution played by mean strain and buoyant effects.

The present recommendations spring from the work of Launder, Reece, and Rodi (1975), Launder (1975B), and Gibson and Launder (1976, 1978). The basic idea is that, due to process (A), the pressure fluctuations will tend to produce a return to isotropy [a proposal due originally to Rotta (1951)] while processes (B) and (C) will diminish the rate of stress creation by shear and buoyancy, respectively.

Thus, for free shear flows we recommend that the pressure-strain correlation be approximated as

$$\overline{\frac{p}{\rho}\left(\frac{\partial u_i}{\partial x_j} + \frac{\partial u_j}{\partial x_i}\right)} = \underbrace{-c_1 \frac{\epsilon}{k}\left(\overline{u_i u_j} - \tfrac{2}{3}\delta_{ij} k\right)}_{\varphi_{ij,1}} \underbrace{- c_2\left(P_{ij} - \tfrac{2}{3}\delta_{ij} P\right)}_{\varphi_{ij,2}} \underbrace{- c_3\left(G_{ij} - \tfrac{2}{3}\delta_{ij} G\right)}_{\varphi_{ij,3}}, \tag{27}$$

where P_{ij} and G_{ij} denote the kinematic generation rate of $\overline{u_i u_j}$ by mean shear and buoyant action, respectively:

$$P_{ij} \equiv -\left\{\overline{u_i u_k}\frac{\partial U_j}{\partial x_k} + \overline{u_j u_k}\frac{\partial U_i}{\partial x_k}\right\}$$

and

$$G_{ij} \equiv -\left(\frac{\overline{\rho' u_j}}{\rho} g_i + \frac{\overline{\rho' u_i}}{\rho} g_j\right),$$

and P and G are the corresponding rates of kinetic-energy generation. Note that, under contraction of indices, the left side of Eq. 27 vanishes in a strictly incompressible turbulent field due to continuity; this characteristic is retained by the approximation on the right, since $\overline{u_i u_i} = 2k$, $P_{ii} = 2P$, and $G_{ii} = 2G$.

In the present work we retain Eq. 27, though in a compressible flow, the contraction of the pressure-strain correlation will not exactly be zero. The quantity k/ε, whose reciprocal appears in the first term on the right of Eq. 27, provides a characteristic time scale for changes to the turbulent velocity field. Its reciprocal (ε/k) thus gives the characteristic rate at which the process in question proceeds; the term as a whole thus tends to drive the turbulent stresses to their isotropic state $[(2/3)\delta_{ij}k]$ at a rate proportional to the level of anisotropy and to the characteristic turbulent change rate. Optimization of c_1 over a range of free shear flows suggests the optimum value to be about 1.8. The coefficients c_2 and c_3 are selected as 0.6 and 0.5 by reference to data of stress ratios in horizontal simple shear layers.

In considering confined flows or external flows along a rigid surface, we must, unfortunately, account for a further aspect of the pressure-strain correlation. The difficulty arises because a wall modifies the fluctuating pressure field; it will reflect pressure fluctuations rather as a mirror reflects light. Most groups working with second-order closures still neglect this effect. Provided one restricts attention to a narrow class of flows (and examines only the predicted mean flow field), this neglect seems acceptable. There is, however, a growing awareness that any general turbulence-model formulation does need to include the wall effects on the pressure-containing correlations.

At present, extensive testing has considered only a simple shear flow past a single plane wall with no gravitational contribution [Launder, Reece, and Rodi (1975); Irwin (1974); Gibson and Launder (1978)]. The present recommendations are taken, with but minor modifications, from the last of these contributions. We denote by $\overline{p(\partial u_i/\partial x_j + \partial u_j/\partial x_i)}_w$ the modification of the pressure-strain correlation due to the wall. This is to be added to the free-flow form, Eq. 27. That is,

$$\underbrace{\overline{p\left(\frac{\partial u_i}{\partial x_j}+\frac{\partial u_j}{\partial x_i}\right)_w}}_{\varphi_{ij,w}} = \left\{c_1'\frac{\epsilon}{k}\left[4\left(\frac{\overline{u_iu_k}\;\overline{u_ju_\ell}}{k}n_kn_\ell - \tfrac{1}{3}\delta_{ij}\,\overline{u_mu_k}\;\overline{u_mu_\ell}\;n_kn_\ell\delta_{ij}/k\right)\right.\right.$$

$$-\left(\overline{u_iu_k}\,n_jn_k + \overline{u_ju_k}\,n_in_k - \tfrac{2}{3}\delta_{ij}\,\overline{u_mu_k}\,n_mn_k\right)\Big]$$

$$- c_2'\left(\varphi_{ik,2}n_jn_k + \varphi_{jk,2}n_in_k - \tfrac{2}{3}\delta_{ij}\varphi_{mk,2}n_kn_m\right)$$

$$\left.- c_3'\left(\varphi_{ik,3}n_jn_k + \varphi_{jk,3}n_in_k - \tfrac{2}{3}\delta_{ij}\varphi_{mk,3}n_kn_m\right)\right\}f_1\left(\frac{k^{3/2}}{\epsilon x_n}\right). \qquad (28)$$

Here x_n is normal distance above the wall and the n's are unit vectors normal to the surface. We propose that the coefficients c_1', c_2', and c_3' should take the values, 0.3, 0.4, and 0.4, respectively. The wall-effect function $f_1(k^{3/2}/\epsilon x_n)$ is in fact taken as linear and equal to unity close to the wall, where $k^{3/2}/\epsilon$ increases linearly with x_n. Thus,

$$f_1\left(\frac{k^{3/2}}{\epsilon x_n}\right) = c_w\frac{k^{3/2}}{\epsilon x_n}, \qquad (29)$$

where c_w takes the value 0.38 so that the function satisfies the above requirement.

The work of Reece (1977) appears to be the only one so far that has attempted to include the effect of more than one wall. As shown in Fig. 1, he assumed that for two walls at right angles, the effects of the two walls could be added linearly without any cross-coupling. For example, if the unit vectors normal to the adjacent surfaces point in the positive x_1 and x_2 directions, the total wall effect at a point P is the sum of two contributions: one arising from wall 1 with a wall-effect function of $c_wk^{3/2}/\epsilon x_1$ and the other, due to wall 2, in which the corresponding wall-effect function is $c_wk^{3/2}/\epsilon x_2$. Of course, for positions that are much closer to one wall than another, the effect of the nearby surface predominates, since $k^{3/2}/\epsilon x_n$ will be so much larger for the closer wall.

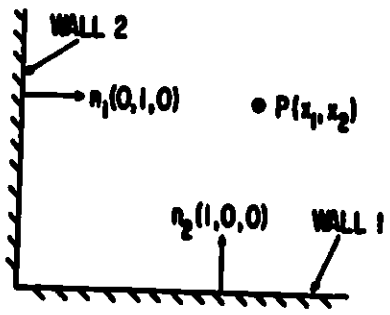

Fig. 1

Two Walls at Right Angles

In general circumstances, i.e., for an arbitrarily contoured boundary, the wall effect should properly be expressed in terms of an integral around the circumference. The details of such a scheme do not, however, seem to have been worked out.

The most important nonplanar case is the circular sectioned pipe or container. At present, for this geometry, the best practice would appear to be to use the formula for the plane-wall correction. Such a practice should lead to a modest overestimate of the circumferential velocity fluctuations at the expense of axial ones; it is, however, rather doubtful that the model for a plane flow is sufficiently accurate for any definite conclusion to be reached about the cause of any discrepancies between data and prediction for, say, fully developed flow in a pipe.

4. Strategy for Closing the Equations for $\overline{u_j\gamma}$

Section II.C.1 presented the main ideas behind the high-Reynolds number modeling of the turbulence velocity field; i.e., the fine-scale viscosity-dependent part of the motion was unaffected by the nature of the large-scale motions and was thus isotropic. Correspondingly, the large-scale motions were unaffected by the fine scale and thus were independent of Reynolds number.

The same state of affairs will also pertain to heat transport, provided the Prandtl number of the fluid is of order of unity greater. For liquid metals, however, because Prandtl numbers are then of order 10^{-2}, there will commonly be no truly fine-scale thermal turbulence and the large-scale temperature fluctuations will be affected by molecular transport. Put another way, the high thermal conductivities mean that heat will leak away from an eddy in transit from one region of flow to another. It is therefore evident that turbulence agitations will be less effective in augmenting heat transport in liquid-metal flows than in other fluids.

Our strategy in closing the heat-flux equation will be to assume that only the most important turbulent correlations are affected and that these are functions only of the local turbulent Peclet number. This approach is almost certainly an oversimplification. When venturing into a nearly unexplored field, however, we find it best to start with a simple model so that the cause of any errors can be easily traced and cured. Moreover, by keeping the model simple, we have much less risk of making a major error.

5. Molecular Dissipation of the Heat-flux Correlation

When the Prandtl number is of order unity or greater, the correlation between derivatives of velocity and temperature, given by term D in Eq. 19, is negligible outside the viscous sublayer and buffer region. Under conditions of low turbulent Peclet number, however, it seems plausible to correlate the process as follows:

$$\epsilon_{j\gamma} = f_{1\gamma}(Pe_t)\overline{u_j\gamma}\sqrt{\epsilon\, e_g/kg}, \tag{30}$$

where $\epsilon_{j\gamma}$ stands for term D in Eq. 19 divided by ρ. The turbulent Peclet number Pe_t is defined as $\rho c_p k^2/\epsilon\lambda$. The functional, $f_{1\gamma}$, should approach zero as Pe_t becomes large (i.e., greater than about 300) and will approach some constant value, of order unity, when the Peclet number becomes very small.

We make no proposals for approximating the function $f_{1\gamma}$ because, as we shall see in the next section, a directly similar term also appears. We shall model the two processes together, thus keeping to a minimum the number of empirical functions to be optimized.

6. Pressure-temperature-gradient Correlation

Process E in Eq. 19 is approximated broadly along the lines proposed by Gibson and Launder (1978), but generalized to include low-Peclet-number effects.

The basic form for flows remote from walls is taken as

$$\overline{\frac{p}{\rho}\frac{\partial\gamma}{\partial x_j}} = \underbrace{-c_{1\gamma}\sqrt{\frac{\epsilon e_g}{kg}}\,\overline{u_j\gamma}}_{\varphi_{j\gamma,1}} - \underbrace{c_{2\gamma}P_{j\gamma}}_{\varphi_{j\gamma,2}} - \underbrace{c_{3\gamma}G_{j\gamma}}_{\varphi_{j\gamma,3}}. \tag{31}$$

The quantities $P_{j\gamma}$ and $G_{j\gamma}$, respectively, stand for the rate of generation of the correlation $\overline{u_j\gamma}$ by mean shear and buoyancy:

$$P_{j\gamma} \equiv -\overline{u_k\gamma}\frac{\partial U_i}{\partial x_k} \tag{32}$$

and

$$G_{j\gamma} \equiv \overline{\rho'\gamma}\, g_j/\rho. \tag{33}$$

The coefficients $c_{2\gamma}$ and $c_{3\gamma}$ are taken as independent of Peclet number.

For isotropic turbulence, we may show [Launder (1975A), Lumley (1975)] that the coefficient $c_{3\gamma}$ should equal exactly 1/3; experiments seem to suggest that, for shear flows, however, a rather larger fraction of the buoyant generation may be obliterated by pressure. Accordingly, we take $c_{3\gamma} = 0.4$ and, noting the basic similarity of the processes, we let $c_{2\gamma}$ take the same value. The coefficient $c_{1\gamma}$ takes a value of about 2.0 at high Peclet numbers, that is, a value similar to that of c_1 for the corresponding part of the pressure-strain correlation.

The cumbersome group $\sqrt{\epsilon\epsilon_g/kg}$ is just the geometric mean of the velocity and thermal turbulent rates of change. It is convenient to rewrite this as $(\epsilon/k)/R^{1/2}$, where R is the time-scale ratio $g\epsilon/k\epsilon_g$. The quantity R is not strictly constant, even at high Peclet numbers; the review by Launder (1976), for example, shows a roughly threefold variation in its magnitude over the relatively small span of flows in which the requisite experimental data are available. Nevertheless, in simple shear, whether close to or remote from a wall, a value close to 0.6 seems to be indicated (Beguier et al., 1978); that is the value we adopt. In the present work we take the view--which is broadly consistent with Lawn's (1977) hypothesis discussed earlier--that the effect of Peclet number on R represents the main source of molecular activity on the turbulent-heat-transport mechanism.

Let us note also that, on adding the molecular-dissipation process (Eq. 30) to $\varphi_{j\gamma,1}$, we obtain

$$\varepsilon_{j\gamma} + \varphi_{j\gamma,1} = -c_{1\gamma}\frac{\epsilon}{k}\overline{u_j\gamma}\underbrace{\left(R^{-1/2} + \frac{R^{-1/2}f_{1\gamma}}{c_{1\gamma}}\right)}_{F_1(Pe_t)}. \tag{34}$$

The quantity $F_1(Pe_t)$ takes the value unity as the local turbulent Peclet number attains large values and takes on very large values as Pe approaches zero (provided the turbulent Reynolds number is high).

The analyses of Deissler (1963) and Corrsin (1952), as well as several empirical correlations, suggest that the turbulent Prandtl number is inversely proportional to the laminar Prandtl number in this limit. It is readily demonstrated that, by neglecting convection and diffusive transport, Eq. 18 does give this inverse relation between molecular and turbulent conductivities, provided F_1 varies as Pe_t^{-1} in the limit as the turbulent Peclet number approaches zero.

It has usually been found, from the work of Van Driest (1956) onward, that exponential functions allow one to fit the dramatic changes in effective transport coefficients across the viscosity-affected region more compactly than do polynomial forms. A disadvantage of using exponentials is that their evaluation takes a significant portion of the total computing time. Once a suitable exponential form has been devised, however, it is easy to make a piecewise linear fit to it--and such piecewise linear functions take only a few percent of the computer time required for the exponentials. Noting the required limiting behavior, we therefore choose

$$F_1 = [1 - \exp(-Pe_t/a)]^{-1}, \tag{35}$$

where the empirical coefficient a should take a value of about 70 to ensure that F_1 differs little from unity when Pe_t is about 300. It may prove necessary

to introduce a more elaborate functional form to give a satisfactory dependence of F_1 on Pe_t at intermediate values of the turbulent Peclet number; this question can only be resolved by computational tests.

7. Near-wall Effects on Pressure-temperature-gradient Correlation

Just as for the pressure-strain correlation discussed above, a general model of heat transport needs to include the way the wall, through reflecting pressure fluctuations, modifies the pressure-temperature-gradient formulation given above. We adopt precisely parallel modeling concepts as used for $\overline{p(\partial u_i/\partial x_j + \partial u_j/\partial x_i)}_w$. We take

$$\left.\overline{p\frac{\partial\gamma}{\partial x_j}}\right|_w = \rho\left[-F_1'\frac{\varepsilon}{k}(c_{1\gamma}'\,\overline{u_k\gamma}\,n_k n_j) - c_{2\gamma}'\varphi_{j\gamma,2} - c_{3\gamma}'\varphi_{j\gamma,3}\right] f_2\left(\frac{k^{3/2}}{\varepsilon x_n}\right). \tag{36}$$

Only Gibson and Launder (1978) appear to have given detailed attention to near-wall effects on $\overline{p\partial\gamma/\partial x_j}$. In their work, the coefficient $c_{1\gamma}'$ took the value 0.5, which is retained here. In the flows considered by Gibson and Launder (1978), since the process $\varphi_{j\gamma,2}$ did not appear, the coefficient c_2' was immaterial. Moreover, in the absence of further evidence to the contrary, $c_{3\gamma}'$ was set to zero. In view of the similarities found so far between the coefficients in the pressure-strain and pressure-temperature-gradient models, we now take the view that it is more consistent to put $c_{3\gamma}'$ equal to c_3' and $c_{2\gamma}'$ equal to c_2'.

We note that the first term on the right of Eq. 36 is much simpler in appearance than the corresponding part of Eq. 28. The reason for this is partly that here we are modeling a tensor of first rank (i.e., a vector), whereas Eq. 28 is a second-rank symmetric tensor. A further reason is that much less is known experimentally about the characteristics required of the model for $\overline{(p\partial\gamma/\partial x_j)}_w$ than that for $\overline{p(\partial u_i/\partial x_j + \partial u_j/\partial x_i)}_w$. The form proposed in Eq. 36 does ensure the basic requirement that the wall should tend to raise the turbulent Prandtl number (for heat fluxes normal to the wall). Perhaps, however, as it becomes clearer what the corresponding effects are on the heat fluxes parallel to the surface, additional nonlinear terms will be needed corresponding to those already retained in the near-wall pressure-strain model.

Following Gibson and Launder (1978), we take the function $f_2(k^{3/2}/\varepsilon x_n)$ equal to $f_1(k^{3/2}/\varepsilon x_n)$ and recommend the same linear-superposition approach used for $\overline{p(\partial u_i/\partial x_j + \partial u_j/\partial x_i)}$ when more than one wall is present.

8. Diffusive Transport

At high levels of turbulent Peclet and Reynolds numbers, it has been customary [see Launder (1976)] to approximate the turbulent diffusion of heat flux as

$$-(\rho\,\overline{u_k u_j\gamma} + \overline{p\gamma}\,\delta_{jk}) = \rho\left(c_{j\gamma}\frac{k}{\varepsilon}\overline{u_k u_\ell}\,\frac{\overline{\partial u_j\gamma}}{\partial x_\ell}\right). \tag{37}$$

More elaborate and physically more realistic versions have been proposed [e.g., André et al. (1976) and Kolovandin (1977)], but these forms add considerably to the computational task without, for the most part, producing a commensurate advance in the accuracy of predictions. The coefficient $c_{j\gamma}$ should take a value close to 0.2.

In all other turbulence-transport equations appearing in this report, molecular-transport terms may be included without further approximation, because the molecular-transport rate is directly proportional to the gradient of the correlation in question. This state of affairs is unfortunately not the case in the turbulent heat-flux equation, as reference to Eq. 19 will show. In the region of high-Reynolds-number turbulence, the term as a whole is of significance only if $Pr << 1$, that is, if $\lambda >> c_p\mu$. Moreover, $\overline{u_j\partial\gamma/\partial x_k}$ will be of the same order as $\overline{\gamma\partial u_j/\partial x_k}$. Thus, from Eq. 19 we may write that

$$\text{Net molecular diffusion rate of } \overline{u_j\gamma} \simeq \frac{\partial}{\partial x_k}\left(\frac{\lambda}{c_p}\overline{u_j\frac{\partial\gamma}{\partial x_k}}\right). \tag{38}$$

$\overline{\lambda u_j\partial\gamma/\partial x_k}$ Current practices in turbulence-model closure would suggest that be modeled in either of the following ways:

$$\overline{\lambda u_j\frac{\partial\gamma}{\partial x_k}} \propto -\lambda\frac{k}{\epsilon}\overline{u_ju_\ell}\frac{\partial^2\Gamma}{\partial x_\ell\partial x_k} \tag{39a}$$

or

$$\overline{\lambda u_j\frac{\partial\gamma}{\partial x_k}} \propto \lambda\partial\overline{u_i\gamma}/\partial x_k. \tag{39b}$$

The former of these leads to third derivatives of mean temperature, and these require a fine mesh to resolve them with accuracy, for this reason, at least the second alternative looks preferable. The constant of proportionality should be about 0.5.

In fact, as discussed in the following section, by taking a rather different approach to modeling transport effects in the stress and heat-flux equations, we can greatly reduce the complexity of our model. For this reason, we do not make definite recommendations for the values of the empirical coefficients appearing in the diffusive terms.

9. Nonstationary Source

The final term in Eq. 19 requiring approximation is term G, which, on division by ρ, becomes

$$\left(1 - \frac{c_v}{c_p}\right)\overline{u_j\frac{\partial\gamma}{\partial t}}. \tag{40}$$

The term will be zero, except in gaseous flows, for only there will c_p and c_v differ. Following the discussion in the previous section, we should approximate the group as

$$\propto \left(1 - \frac{c_v}{c_p}\right)\overline{\frac{\partial u_i \gamma}{\partial t}}, \tag{41}$$

where the constant of proportionality should be about 0.5. In the final form of the turbulence model we shall, however, regard term 40 as part of the convective transport of $\overline{u_j\gamma}$ and will approximate it in terms of the convective transport of k and g as discussed next.

D. Algebraic Stress Modeling

1. Stress and Scalar Flux Formulas

"Algebraic Stress Modeling" (ASM) is the name given to closures derived from stress-transport models in which all the transport effects are held to be characterizable in terms of scalar properties of the turbulence field. Because gradients of stresses and heat fluxes appear (according to present closure ideas) only in the transport terms, the resultant equations for the Reynolds-stress and heat-flux equations are algebraic ones. Transport equations are needed just for the scalar quantities; the great saving in computer memory required has already been discussed. Following Rodi (1972), we take

$$T_{ij} = \frac{\overline{u_i u_j}}{k} T_k, \tag{42}$$

where T denotes net transport rate (i.e., convection minus diffusion) and the subscripts ij and k denote that the transports of $\overline{u_i u_j}$ and of k, respectively, are in question.

Now the turbulence-kinetic-energy equation may, in symbolic notation, be written

$$T_k = P + G - \epsilon. \tag{43}$$

Thus, Eq. 42 may be rewritten

$$T_{ij} = \frac{\overline{u_i u_j}}{k}(P + G - \epsilon). \tag{44}$$

In considering heat-transport processes, Gibson and Launder (1978) have similarly assumed that

$$T_{j\gamma} = \frac{\overline{u_j\gamma}}{k^{1/2}g^{1/2}} T \sqrt{g}\sqrt{k} \,. \tag{45}$$

Now, formally,

$$T \sqrt{g}\sqrt{k} = \frac{1}{2}\left(\frac{k^{1/2}}{g^{1/2}} T_g + \frac{g^{1/2}}{k^{1/2}} T_k\right). \tag{46}$$

Thus, Eq. 45 may be rewritten

$$T_{j\gamma} = \tfrac{1}{2}\overline{u_j\gamma}\left(\frac{1}{g} T_g + \frac{1}{k} T_k\right) = \frac{\overline{u_j\gamma}}{2}\left(\frac{P_g - \epsilon_g}{g} + \frac{P + G - \epsilon}{k}\right). \tag{47}$$

Finally, we eliminate ϵ_g in favor of the time-scale ratio $R[\equiv (g\epsilon/\epsilon_g k)]$. The following final expression is thus obtained for $T_{j\gamma}$:

$$T_{j\gamma} = \frac{\overline{u_j\gamma}}{2}\left[\frac{P_g}{g} + \frac{P + G}{k} - \frac{\epsilon}{k}\left(1 + \frac{1}{R}\right)\right]. \tag{48}$$

The production terms in Eqs. 44 and 48 may be regarded as known.

The stress and heat-flux transport approximations thus depend on four scalar properties of turbulence. The values of three of these (k, ϵ, and g) are obtained from transport equations given below; the time-scale ratio R is prescribed as a function of the turbulent Peclet number, as discussed in Sec. II.C.6 above and specifically as given by Eq. 54 below.

With Eqs. 44 and 48 used to approximate the transport of $\overline{u_iu_j}$ and $\overline{u_j\gamma}$, the closure proposals presented in Sec. II.C may be manipulated to give the following algebraic formulas for the turbulent stress and heat-flux fields:

$$\overline{u_iu_j} = \frac{k}{\epsilon}\left[(c_1 - 1) + \frac{P + G}{\epsilon}\right]^{-1}\left[P_{ij} + G_{ij} - c_2(P_{ij} - \tfrac{2}{3}\delta_{ij}P) - c_3(G_{ij} - \tfrac{2}{3}\delta_{ij}G)\right.$$
$$\left. + \varphi_{ij,w} + \tfrac{2}{3}(c_1 - 1)\epsilon\delta_{ij}\right], \tag{49}$$

where $\varphi_{ij,w}$ stands for the wall effect on the pressure-strain correlation expressed by Eqs. 28 and 29, and

$$\overline{u_j\gamma} = 2\left\{\frac{P_g}{g} + \frac{P + G}{k} - \frac{\epsilon}{k}\left[1 + \frac{1}{R} - c_{1\gamma}F_1(Pe)\right]\right\}^{-1}\left[-\overline{u_ju_k}\,\partial\Gamma/\partial x_k + (1 - c_{2\gamma})P_{j\gamma}\right.$$
$$\left. + (1 - c_{3\gamma})G_{j\gamma} + \varphi_{j\gamma,w}\right]. \tag{50}$$

The quantity $\varphi_{j\gamma,w}$ is the wall effect on the pressure-temperature-gradient correlation modeled by Eq. 36.

The above equations provide the central constitutive relations for calculating the stresses and heat fluxes from a knowledge of the scalar properties k, ϵ, and g, quantities that are obtained from the transport equation for these variables given below.

2. Modeling the Transport of the Scalar Properties of Turbulence

The ASM closure of Sec. II.D.1 contains as unknowns the kinetic and scalar energies of turbulence (k and g) and their respective dissipation rates (ϵ and ϵ_g).

Exact equations for the transport of k and g were presented in Sec. II.B (Eqs. 20 and 21). If we adopt the gradient-transport notion for modeling the diffusion of turbulence energy, Eq. 20 may be written as

$$\rho\frac{\partial k}{\partial t} + \rho U_k\frac{\partial k}{\partial x_k} = \rho P + \rho G - \rho\epsilon + c_s\frac{\partial}{\partial x_k}\left(\rho\overline{u_k u_\ell}\frac{k}{\epsilon}\frac{\partial k}{\partial k_\ell}\right), \tag{51}$$

where the coefficient c_s is the same as in Eq. 25; the recommended value is 0.22. Generation rates P and G contain only (1) mean field variables and the Reynolds stresses and (2) heat fluxes, respectively, and may be regarded as known; the local level of ϵ is to be obtained from Eq. 53 below. Equation 51 may thus be regarded as closed.

Correspondingly, the scalar energy-transport equation may be written

$$\rho\frac{\partial g}{\partial t} + \rho U_k\frac{\partial g}{\partial x_k} = \rho P_g - \rho\frac{\epsilon g}{kR} + c_g\frac{\partial}{\partial x_k}\left(\rho\frac{k}{\epsilon}R^{1/2}\overline{u_k u_\ell}\frac{\partial g}{\partial x_\ell}\right) + \frac{\partial}{\partial x_k}\left(\frac{\lambda}{c_p}\frac{\partial g}{\partial x_k}\right), \tag{52}$$

where P_g is the creation rate of temperature fluctuations, $-\overline{u_k\gamma}\partial\Gamma/\partial x_k$, and, in place of the molecular dissipation rate of temperature fluctuations, ϵ_g, we have, as in Sec. II.C.5, introduced the time-scale ratio R. We have also included this dimensionless time scale in the model for the turbulent diffusive transport of g (the third term on the right-hand side of Eq. 52) to reflect the fact that temperature fluctuations are being diffused. There seems about as much justification for an exponent of R of 2/3 as 1/2, but the question is unlikely to be of much practical significance. Only at low turbulent Peclet numbers will R become sufficiently small for there to be a substantial difference between $R^{1/2}$ and $R^{2/3}$, and, in this case, turbulent diffusion will probably be outweighed by molecular diffusion, represented exactly by the fourth term on the right of Eq. 52.

3. Modeling the Transport of Energy-dissipation Rate

An exact equation for the turbulence-energy dissipation rate ϵ may be obtained by taking the derivative of the fluctuating velocity equation, Eq. 15, with respect to x_k and multiplying through by $2\nu(\partial u_i/\partial x_k + \partial u_k/\partial x_i)$. The resultant equation has been presented by Daly and Harlow (1970) and

discussed by the same workers, by Hanjalić and Launder (1972), by Lumley and Khajeh Nouri (1974), and by several others. Tennekes and Lumley (1972) brought out the difficulty of devising a closed form for the ϵ transport equation in their discussion of the closely related turbulent-vorticity equation. It turns out that none of the terms in the equation are accessible to measurement. In these circumstances, the only feasible approach toward devising a modeled ϵ equation is to apply a mixture of intuition and intelligent dimensional analysis. The conjectured form of the equation should contain a number of empirical coefficients that may be tuned by reference to the behavior of widely different shear flows. The form proposed here is essentially that of Launder, Reece, and Rodi (1975):

$$\rho\frac{\partial\epsilon}{\partial t} + \rho U_k\frac{\partial\epsilon}{\partial x_k} = c_{\epsilon 1}\rho\frac{\epsilon}{k}P + c_{\epsilon 3}\rho\frac{\epsilon G}{k} - c_{\epsilon 2}\rho\frac{\epsilon^2}{k} + c_\epsilon\frac{\partial}{\partial x_k}\left(\rho\frac{k}{\epsilon}\overline{u_k u_\ell}\frac{\partial\epsilon}{\partial x_\ell}\right). \qquad (53)$$

Following Launder, Reece, and Rodi (1975), the coefficients $c_{\epsilon 1}$, $c_{\epsilon 2}$, and c_ϵ are assigned the values 1.44, 1.90, and 0.15, respectively. The term containing $c_{\epsilon 3}$ did not appear in that work, since its authors were concerned exclusively with unstratified flows. Gibson and Launder (1978) obtained good results by making $c_{\epsilon 3}$ zero; Ideriah (1976) and Hossain and Rodi (1977) found it necessary to make $c_{\epsilon 3}$ nonzero to correctly predict the size of the round buoyant plume. However, while Hossain and Rodi took the value of $c_{\epsilon 3}$ the same as $c_{\epsilon 1}$, Ideriah deduced its magnitude to be only about half that value. We can provide arguments in favor of either choice, but neither is especially convincing. On the grounds of simplicity, $c_{\epsilon 3} = c_{\epsilon 1}$ is preferable since this says that it is the <u>total</u> generation of turbulence energy that matters, irrespective of whether it is due to shear or buoyant action. This is the practice we recommend at present.

For a number of years, Lumley and his colleagues [e.g., Lumley (1972), Siess (1975), and Zeman and Lumley (1977)] have been making proposals for a corresponding transport equation for ϵ_g. The exact equation is similar in structure to that for ϵ, and, not surprisingly therefore, the modeled forms likewise show close kinship. Launder (1976) pointed out that the task of closing the ϵ_g equation appears rather <u>more</u> difficult than for the ϵ equation, because there are now <u>two</u> turbulent times scales (k/ϵ and g/ϵ_g) and two length scales available for devising dimensionally correct forms. As Launder (1976) remarks, "All the published modeled forms of the ϵ_g equation ... are at best tentative." Though recognizing the <u>desirability</u> of determining ϵ_g from its own transport equation, it appears to us at present to involve greater uncertainty and empiricism than the alternative of prescribing the time-scale ratio R. (This state of affairs will probably change in the next year or two.)

As discussed in Sec. II.C, values of R deduced from turbulence studies suggest values ranging from about 1/3 to unity, with a preponderance of values in the range 0.5-0.7. We chose an asymptotic value for R of 0.7 because, as reported by Launder (1976), a value as low as 0.5 produces apparently quite the wrong effect of buoyancy on the effective turbulent Prandtl number.

Of course the effect of molecular heat transport on R is substantial. We have already considered modeling the Peclet-number dependence of a function in which R appears (Eq. 24). The tentative modeled form of that equation suggests that R itself should be approximated as

$$R = 0.7[1 - \exp(-Pe_t/a')]^2, \tag{54}$$

where the empirical coefficient a' should be of about the same magnitude as the constant a appearing in Eq. 35 (but not necessarily exactly the same due to the presence of $f_1 \cdot \gamma$ in Eq. 34, for which Eq. 35 is also supposed to account).

4. Closure

Sections II.D.1-II.D.3 have presented the algebraic stress model currently recommended for computing three-dimensional recirculating flows. For internal flows, the stress and heat-flux correlations must be used in conjunction with the near-wall corrections, Eqs. 28 and 36.

The recommended values of the empirical coefficients have mostly been stated as the coefficients appeared in the equations; for convenience, however, they are restated in Table I. The greatest uncertainty concerns the Peclet-number dependence of the time-scale ratio and the associated function $F_1(Pe_t)$ in the heat-flux equation. Additional work is needed to refine and validate the present proposals.

TABLE I. Values of Various Coefficients

Coefficient or Function	Value (or Form) Proposed	Equation of First Appearance	Basis for Choice
c_1	1.8	27	Stress levels in free shear flows
c_2	0.6	27	
c_3	0.5	27	Gravitational effects on horizontal free shear flows
c_s ($c_k = c_s$)	0.22	25	Computer optimization (see Launder et al. 1975)
c_1'	0.3	28	Normal stress levels in near-wall turbulence
c_2'	0.4	28	
c_3'	0.4	28	Buoyant effects on stress levels in atmospheric boundary layer
c_w	0.38	29	Near-wall turbulence data
$c_{1\gamma}$	2.5	31	Heat flux in thin shear flows near local-equilibrium
$c_{2\gamma}$	0.4	31	
$c_{3\gamma}$	0.4	31	Heat flux levels in buoyancy-affected horizontal shear flows
$c_{j\gamma}$	0.20	37	Computer optimization
$F_1(Pe_t)$	$1 - \exp(-Pe_t/a)]^{-1}$, $a = 70$	34	Tentative form
$c_{1\gamma}'$	0.5	36	Prandtl number in near wall turbulence
$c_{2\gamma}'$	0.4	36	Equality with c_2'
$c_{3\gamma}'$	0.4	36	Equality with c_3'
c_g	0.15	52	Analogy with c_ε
c_ε	0.15	53	Computer optimization (LRR)
$c_{\varepsilon 1}$	1.44	53	Computer optimization (LRR)
$c_{\varepsilon 2}$	1.90	53	Computer optimization (LRR)
R	$0.7[1 - \exp(-Pe_t/a)]^2$, $a = 70$	54	Tentative proposal

III. BOUNDARY CONDITIONS FOR TURBULENCE PARAMETERS

A. Preliminary Remarks

We consider here the prescription of boundary values for the three scalar quantities whose magnitudes are found from the transport equations presented in Sec. II.D. Three boundary conditions are considered: a plane (or axis) of symmetry, a free boundary, and a wall. The first two are easily dealt with and are presented first; most of the section is concerned with how to apply boundary conditions at a wall.

B. Flow Inlet and Outlet Boundaries and Axes or Planes of Symmetry

At an inlet section, the level of the turbulence quantities depends upon what has happened to the flow at positions upstream of the inlet plane. For this reason, no generally valid prescriptions can be given. Ideally, we would like to have experimental data to turn to; in practice, however, detailed turbulence measurements are limited to rather simple configurations--considerably simpler than usually found in practical situations.

In the absence of more definite information, the levels of k, ϵ, and g may be obtained from one of the following schemes:

1. When mean profiles of velocity and temperature at inlet are known or can be guessed

Let us suppose that the inlet plane is a surface of constant x and that velocities are significant only in the direction normal to this surface. The inlet turbulence energy may be estimated from

$$k = 3\ell_m^2\left[\left(\frac{\partial U}{\partial y}\right)^2 + \left(\frac{\partial U}{\partial z}\right)^2\right] \tag{55}$$

and the turbulence-energy dissipation rate from

$$\epsilon = k^{3/2}/3^{1.5}\ell_m, \tag{56}$$

where ℓ_m (essentially Prandtl's mixing length) is equal to the smaller of $0.42x_n$ or 0.1δ, where x_n denotes the distance to the nearest wall and δ denotes the width of the shear flow (perhaps half the width of the inlet duct if turbulent mixing extends throughout the duct). The corresponding value for g is given by

$$g = 3.5R\ell_m^2\left[\left(\frac{\partial \Gamma}{\partial y}\right)^2 + \left(\frac{\partial \Gamma}{\partial z}\right)^2\right]. \tag{57}$$

2. When uniform inlet values of velocity and temperature are prescribed

In this case, Eq. 55 indicates that the level of turbulence energy is zero. In practice, however, there will always be some residual level of turbulent-velocity fluctuations. How much will depend on the upstream flow configuration. A fairly safe middle-of-the-road estimate would be

$$k = 10^{-3}U^2_{inlet} \tag{58}$$

The dissipation rate ϵ may then be computed from Eq. 56.

If all the upstream surfaces are in thermal equilibrium with the fluid, it will be appropriate to make g equal to zero. At outlet planes, we recommend that zero gradient of turbulence quantities in the flow direction be assumed. At a plane or axis of symmetry, the gradients of k, g, and ϵ normal to the plane (or axis) should be set to zero.

C. Near-wall Boundary Conditions

1. The Basic Model

In the immediate vicinity of a rigid boundary, the levels of all three scalar parameters are strongly modified by molecular effects. The nature of these low-Reynolds-number interactions is, however, very incompletely understood. Moreover, it would be quite beyond the core capability of present-day computers to make three-dimensional finite-difference computations in which the grid extended all the way to the wall. The reason is that the turbulence properties change so rapidly in the region that an extremely fine grid would be needed.

Instead, boundary conditions are devised in terms of the values of the scalar parameters outside the viscosity-dependent region. Our model of the near-wall region can be explained by reference to Fig. 2. This shows a region immediately adjacent to a wall. The node of the finite-difference grid adjacent to the wall is labeled P, and the one next to that NP. We imagine that the level of kinetic energy, velocity, and scalar energy will be found by satisfying their respective transport equation, in the mean, over some designated control volume as shown. We assume that the control-volume boundary between nodes P and NP bisects the line connecting them. Note that within the control volume enclosing node P, two flow regions are present: a fully turbulent region and a sublayer affected by viscosity. For convenience, we shall assume that, for all wall-adjacent control volumes, the node itself lies in the fully turbulent region.

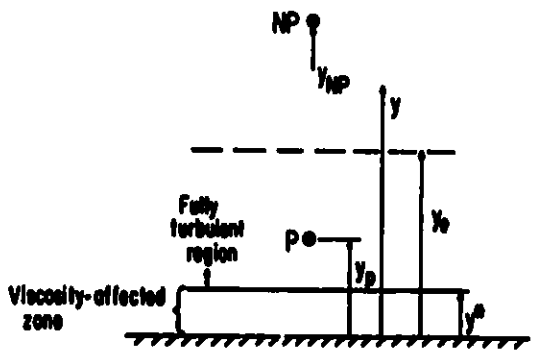

Fig. 2. Model of Near-wall Region

The following simple physical model of this region is envisioned. In the fully turbulent zone, viscous transport effects are negligible (but molecular heat transport may be assumed significant). The thickness of the viscosity-affected region, y*, is such that the turbulent Reynolds number at the edge of the region is a constant:

$$\frac{y^* k^{*1/2}}{\nu} \equiv R_t^*.$$

We take the value of R_t^* to be 20, which corresponds with a "laminar sublayer thickness" of about $11\nu/\sqrt{\tau_w/\rho}$ in local-equilibrium turbulence.

2. Energy-dissipation Rate

The value of ϵ in the near-wall region will be found by expressing it in terms of the kinetic energy and certain other parameters. Unlike the other variables, therefore, the ϵ equation will not be solved for node P.

We make the basic conjecture that, in the fully turbulent region, the length scale near the wall increases linearly with distance from the surface; that is,

$$\ell = c_\ell y, \tag{59}$$

where c_ℓ is assumed to be a universal constant equal to 2.5. The dissipation is then obtained as

$$\epsilon = k^{3/2}/\ell. \tag{60}$$

In fact, the energy-dissipation rate is needed in the P control volume for two different purposes. First, it is needed in order to make a finite-difference approximation of the diffusion rate of ϵ into the NP control volume (which according to our model, will be proportional to $\epsilon_P - \epsilon_{NP}$). In this case, ϵ_P is, from Eq. 60, replaced by $0.4k_P^{3/2}/y_P$. A second and more important role for ϵ is as a negative source term in the turbulence-energy equation.

Now, as explained in the next section, the level of k_P is to be obtained by integrating the turbulence-energy equation over the P control volume. Thus we shall need a value of the mean level of ϵ over the cell. Since ϵ varies so nonlinearly, the use of the point value ϵ_P may lead to serious errors. Instead, in the kinetic-energy equation for the near-wall region, we take the mean dissipation rate over the control volume to be

$$\bar{\epsilon} \equiv \frac{1}{y_e} \int_0^{y_e} \epsilon \, dy, \tag{61}$$

where y_e is the value of y at the edge of the cell. [Note, since the cell edge bisects the line connecting P and NP, $y_e = (y_P + y_{NP})/2$.]

To evaluate $\bar{\varepsilon}$, we first assume that in the viscosity-affected sublayer, the level of ε is constant and equal to $2\nu(dk^{1/2}/dy)^2$, a result derived first by Jones and Launder (1972). We assume that $k^{1/2}$ varies linearly in the viscous region from zero at the wall to $k^{*1/2}$ at the edge of the sublayer. It therefore follows that

$$\varepsilon \equiv \frac{2\nu k^*}{y^{*2}}. \tag{62}$$

We further assume that, in the fully turbulent region, k varies much more slowly over the P control volume than does ε and that we may thus take the level of k at y_P as a representative value from which to find ε; i.e.,

$$\varepsilon \equiv k_P^{3/2}/c_\ell y.$$

The mean value of ε may thus be evaluated as

$$\bar{\varepsilon} \equiv \frac{1}{y_e}\left[\int_0^{y^*} \frac{2\nu k^*}{y^{*2}}\,dy + \int_{y^*}^{y_e} (k_P^{3/2}/c_\ell y)dy\right]$$

$$\equiv \frac{1}{y_e}\left[2\,\frac{k^{*3/2}}{R_t^*} + \frac{k_P^{3/2}}{c_\ell}\,\ell n(y_e/y^*)\right]. \tag{63}$$

The relative importance of the two contributors to $\bar{\varepsilon}$ depends on how thick the viscous sublayer is relative to the cell dimension. In the limit, where node P is only just outside the viscous region, $\ell n(y_e/y^*)$ will be about 0.7; thus, for the recommended values of R_t^* and c_ℓ (20 and 2.5, respectively), the first term contributes a little more than one-quarter of the total. As y^* becomes progressively smaller than y_P, the relative contribution of the dissipation in the viscous sublayer slowly decreases.

3. Turbulent Kinetic Energy

The level of turbulence kinetic energy at node P is obtained from an integration of the transport equation for k over the near-wall cell, neglecting convective transport. (Convective-transport terms may be retained at the expense of algebraic simplicity. Then the left-hand side of Eq. 64 should contain a finite-difference form of the convective flux of kinetic energy per unit mass. For stability, upwind differencing should be used.) To keep the formulation simple, we assume that

a. The velocity parallel to the surface U is planar over the control volume.

b. For evaluating the rate of shear production of turbulence energy, the turbulent shear stress is taken equal to the wall stress in the fully turbulent region and zero in the viscous sublayer.

c. Gravitational contributions to turbulence-energy creation or destruction are negligible.

The last assumption, while perhaps appearing to be too sweeping, will usually be valid because the shear creation terms will generally be largest at the wall, masking the effects of the gravitational contribution. It also follows that, since we have taken

$$k = k^* y^2 / y^{*2}$$

across the viscous sublayer, the diffusion rate of k into the wall (proportional to $\partial k/\partial y$ at $y = 0$) is zero. The kinetic-energy balance for the near-wall cell thus becomes

$$0 = \left|\frac{\tau_w}{\rho}(U_e - U^*)\right| - \bar{\epsilon} y_e + c_s\left(\frac{\overline{v^2}k}{\epsilon}\right)\frac{k_{NP} - k_P}{y_{NP} - y_P}. \tag{64}$$

In the above equation, $\bar{\epsilon}$ is given by Eq. 63 and the group $\overline{v^2}k/\epsilon$ is to be evaluated at the boundary between the NP and P control volumes; $\overline{v^2}$ is the Reynolds normal stress acting in the y direction. The evaluation of U^* is discussed in Sec. III.C.5 below. It will be convenient to eliminate k^* in favor of k_P and k_{NP}. The procedure to be followed is suggested in Fig. 3; k^* is the level of kinetic energy obtained by extrapolating the line through k_P and k_{NP} to $y = y^*$.

Thus

$$k^* = k_P + \frac{y_P - y^*}{y_{NP} - y_P}(k_P - k_{NP}), \tag{65}$$

where

$$y^* = \nu R_t^*/k^{*1/2}.$$

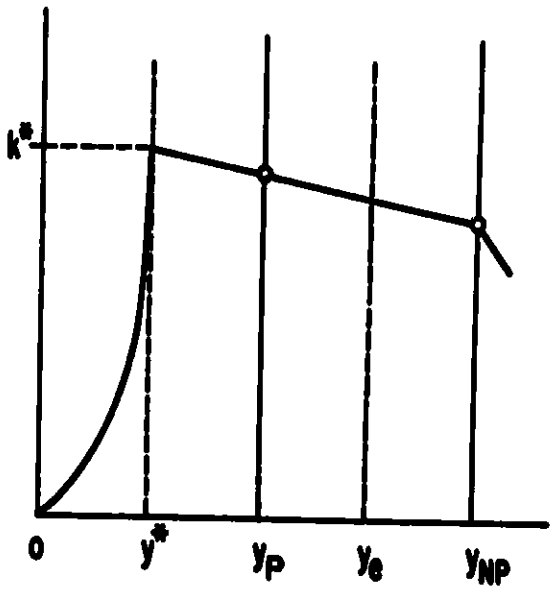

Fig. 3
Model of Near-wall Kinetic-energy Profile

4. Scalar Energy, g

The scalar energy is obtained by following a similar path to that for the turbulence kinetic energy. The problem is somewhat complicated by the importance of molecular heat transport throughout the near-wall cell if we are dealing with liquid metals. Indeed, with the present simple near-wall treatment, we must adopt two distinct near-wall models according to whether the fluid's Prandtl number is of order one or greater or of order 10^{-2} or less. Since the former case parallels almost exactly the treatment for kinetic energy, this is presented first.

a. For Prandtl Numbers of Order 1 or Greater. We assume that molecular effects on g are negligible beyond $y = y^*$ and that, in the fully turbulent region, the normal heat flux, $-\rho c_p \overline{v\gamma}$, is equal to the wall heat flux. We assume also that the level of $\bar{\epsilon}_g$ may be approximated as

$$\bar{\epsilon}_g = \bar{\epsilon} g_P/(k_P R). \tag{66}$$

The above approximation is not strictly consistent with the concept presented in Sec. II.D, for Eq. 54 indicates ϵ/ϵ_g is a function of Prandtl number in the viscous sublayer. Consequently, $\bar{\epsilon}_g/\bar{\epsilon}$ should also be dependent on Prandtl number. Nevertheless, we retain Eq. 66 in the belief that the level of error thereby introduced is not serious for gases or fluids with Prandtl numbers below about 10.

The g-balance equation (again neglecting convective transport) thus takes the form

$$0 = -\frac{\dot{q}''_w}{\rho c_p}(\Gamma_e - \Gamma^*) - \bar{\epsilon} g_P y_e/(k_P R) + \left(c_g \frac{k\overline{v^2} R^{1/2}}{\epsilon} + \lambda/\rho c_p\right)\frac{g_{NP} - g_P}{y_{NP} - y_P}, \tag{67}$$

where $\dot{q}''_w$ represents the local heat flux from the wall into the fluid. As in the kinetic-energy equation, $k\overline{v^2}/\epsilon$ is evaluated at the interface between the P and NP control volumes and R may be taken as its high-Reynolds-number asymptote, 0.7. The evaluation of Γ^*, the temperature at the edge of the viscous sublayer, is considered in Sec. II.C.6 below.

b. For Prandtl Numbers of Order 10^{-2} or Less. In this case, we again approximate the mean value of ϵ_g by Eq. 66. Only now it will be important to evaluate R from its constitutive equation (Eq. 54). The turbulent heat flux is now by no means equal to the wall flux. We thus take the total creation rate of g over the cell equal to $(\Gamma_e - \Gamma^*)$ times the value of $\overline{v\gamma}_P$ produced by the master heat-flux equation (Eq. 50). Thus,

$$0 = -\overline{v\gamma}_P(\Gamma_e - \Gamma^*) - \frac{\bar{\epsilon}\gamma_e g_P}{\bar{k}_P \bar{R}_P} + \left(c_g \frac{k\overline{v^2}R^{1/2}}{\epsilon} + \frac{\lambda}{\rho c_p}\right)\frac{g_{NP} - g_P}{y_{NP} - y_P}. \tag{68}$$

Notice that the molecular thermal diffusivity may now be of substantial importance in calculating the rate of diffusion of g into or out to cell P.

5. Near-wall Velocity Profile and a Drag Law

In applying the momentum equation(s) for directions parallel to the wall to the control volumes adjacent to the surface, we need an expression for the wall shear stress produced for a given velocity U_P at a height y_P. For this purpose, we use a modified version of the "law of the wall" presented by Launder and Spalding (1974), though certain adaptations will be made in the present work.

In the fully turbulent region of flow, where node P is located, we assume the velocity profile to be given by

$$\frac{U}{\tau_{w/\rho}} k^{1/2} = \frac{1}{\kappa^*} \ell n\left(\frac{yk^{1/2}}{\nu} E^*\right), \tag{69}$$

where κ^* is assumed to be a universal constant equal to about 0.23. (This corresponds with a value of the Von Karman constant κ of 0.42.) The constant E^* is obtained as described below. Equation 69 may obviously be arranged to provide the following expression for the wall friction in terms of the value at P:

$$\tau_{w/\rho} = \kappa^* U_P k_P^{1/2} / \ell n(E^* y_P k_P^{1/2}/\nu). \tag{70}$$

We assume further that the velocity profile across the viscous sublayer is linear and given by

$$\frac{Uk^{1/2}}{\tau_{w/\rho}} = \frac{yk^{1/2}}{\nu}. \tag{71}$$

The dimensionless quantity E^* is fixed by requiring that the velocities given by Eqs. 71 and 69 should be the same at the edge of the viscous layer, i.e., at $y = y^*$. That is,

$$\frac{1}{\kappa^*} \ell n(R_t^* E^*) = R_t^*, \tag{72}$$

which, for $\kappa^* = 0.23$ and $R_t^* = 20$, gives $E^* = 4.9$. We note, moreover, that U^* appearing in Eq. 64 is given by

$$U^* = R_t^*(\tau_{w/\rho})/k^{*1/2}. \tag{73}$$

6. Temperature Profile and Wall Heat-flux Relationships

Again different practices are developed, according to whether the Prandtl number is large or small.

a. Prandtl Number of Order 1 or Greater. In this situation, the so-called "universal temperature profile" is used in a form similar to that presented by Jayatilleke (1967)

$$\frac{\rho k_P^{1/2} c_p (\Gamma_w - \Gamma_P)}{\dot{q}''_w} = 0.9\left(\frac{U_P k_P^{1/2}}{\tau_{w/\rho}} + \mathcal{P}\right), \tag{74}$$

which, on cross-multiplying produces the heat-flux relation

$$\dot{q}''_w = \frac{\rho k_P^{1/2} c_p (\Gamma_w - \Gamma_P)}{0.9\left(\frac{U_P k_P^{1/2}}{\tau_{w/\rho}} + \mathcal{P}\right)}, \tag{75}$$

where $$\mathcal{P} = 16.8[1 - (0.9/Pr)^{3/4}]. \tag{76}$$

On evaluating Eq. 74 at the edge of the viscous sublayer, we obtain

$$\Gamma^* = \Gamma_w - 0.9\dot{q}''_w(R_t^* + \mathcal{P})/\rho k^{*1/2} c_p. \tag{77}$$

This expression may be used to eliminate Γ^* in Eq. 67.

b. Prandtl Number of Order 10^{-2} or Less. In this case, we assume that the true temperature profile between the wall and node P departs only slightly from linear, i.e., that turbulent transport of heat makes only a minor contribution in the wall-adjacent control volumes. The heat flux may be expressed by either

$$\dot{q}''_w = -\lambda(\Gamma^* - \Gamma_w)/y^* \tag{78}$$

or

$$\dot{q}''_w = -\lambda(\Gamma_e - \Gamma^*)/(y_e - y^*) + \rho c_p \overline{v\gamma}_P. \tag{79}$$

The latter is conveniently used in Eq. 69 to eliminate $\Gamma_e - \Gamma^*$, while by combining Eqs. 78 and 79, Γ^* may be eliminated to give

$$\dot{q}''_w = [-\lambda(\Gamma_e - \Gamma_w) + \rho c_p \overline{v\gamma}_P (y_e - y^*)]/y_e. \tag{80}$$

This provides the wall heat-flux relationship required in the mean-flow enthalpy equation.

IV. SOME APPLICATIONS OF THE PROPOSED TURBULENCE CLOSURE

A. Preliminary Remarks

Strictly, no computer solutions using the model of turbulence described in Sec. II have yet been reported. The model presented here can, however, be regarded as an extension and refinement of the widely used two-equation closure schemes. Except for liquid-metal flows (for which, in any event, no computations have been made), the model bears close similarity with those reported by Launder (1975), Gibson and Launder (1976, 1978), Hossain and Rodi (1977), and Tamanini (1975). The main difference between the present scheme and those models (apart from the provisions for low Peclet numbers) is the inclusion of a transport equation for the scalar energy. (In all the cited papers except that of Hossain and Rodi, g was obtained by assuming local equilibrium; i.e., $g = P_g(k/\epsilon)R$. Hossain and Rodi, however, took transport effects on the Reynolds stresses and heat fluxes to be entirely zero.) This scheme should never lead to worse agreement than when the more rudimentary treatment of the scalar energy used in other schemes is used.

It is therefore legitimate to form an impression of the kinds of flow that may be successfully tackled with the present scheme by reference to a selection of the flows studied with these closely similar models. Such a comparison is made in the following sections.

B. Velocity and Temperature Fields in Neutral, Thin Shear Flows

Gibson and Launder (1976) report the application of the model to the prediction of the plane jet and the plane mixing layer. Table II, taken from

TABLE II. Comparison of Calculated Results and Experimental Data for Spread of Free Shear Flows

Flow	Growth Rate	Calculated	Data	Data Sources
Plane jet	$\frac{db_u}{dx}$	0.112	0.096, 0.120, 0.096	Data from sources quoted by Jenkins and Goldschmidt (1973)
	$\frac{db_T}{dx}$	0.138	0.137, 0.170, 0.141	
Plane mixing layer				
Velocity ratio 0	$\frac{db_u}{dx}$	0.147	0.130, 0.150, 0.160, 0.20, 0.165	Data from sources quoted by Rodi (1972)
Velocity ratio 0.51	$\frac{db_u}{dx}$	0.044	0.046	
	$\frac{db_T}{dx}$	0.047	0.051	Watt (1967)

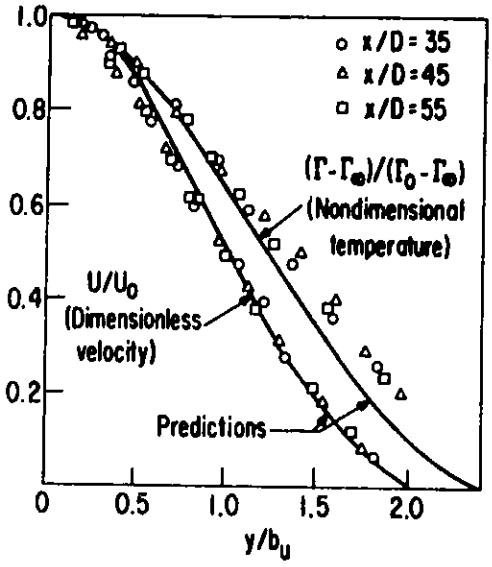

Fig. 4. Mean Velocity and Temperature Profiles in a Self-preserving Plane Jet in Stagnant Surroundings (b_u half-width of the velocity profile)

their paper, shows the measured and predicted rates of spread of the velocity and temperature field. There is generally close agreement between the predicted and measured behavior, except that experiments show a greater difference between the spreading rate of the thermal and velocity layers than do the predictions. This emerges clearly in Fig. 4, which shows temperature and velocity profiles for the plane turbulent jet, the experiments being those of Jenkins and Goldschmidt (1973). The present closure will, in fact, produce closer agreement with the temperature field than in the Gibson-Launder predictions, due to a reduction of the coefficient $c_{1\theta}$ from 3.2 (used by Gibson and Launder) to 2.5.

Samaraweera (1978) applied the present model to thermal boundary layers and to pipe flows. Figure 5 is an example of his predictions for a thin thermal boundary layer developing within a thick velocity boundary layer. A generally satisfactory agreement with experiment is displayed.

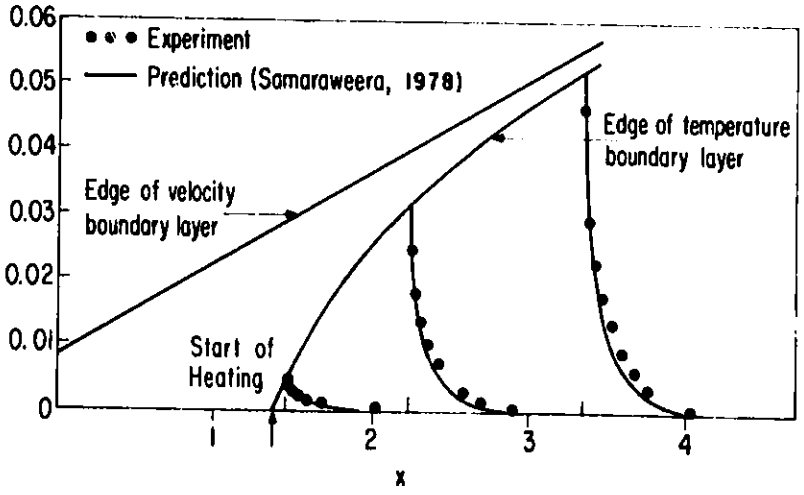

Fig. 5. Development of Thermal Turbulent Boundary Layer on Flat Plate

C. Buoyant Shear Layers

Figure 6 [Gibson and Launder (1976)] shows the predicted development of a plane jet of warm water discharged onto the surface of still cool water (for example, a lake). Initially, the jet grows linearly at the same rate as an isothermal jet. Dynamic forces in the jet, however, die out much faster than buoyant forces. After some distance, the latter (while not exceeding about 25% of the former) greatly reduce the spreading rate, due to a substantial reduction in turbulent agitation.

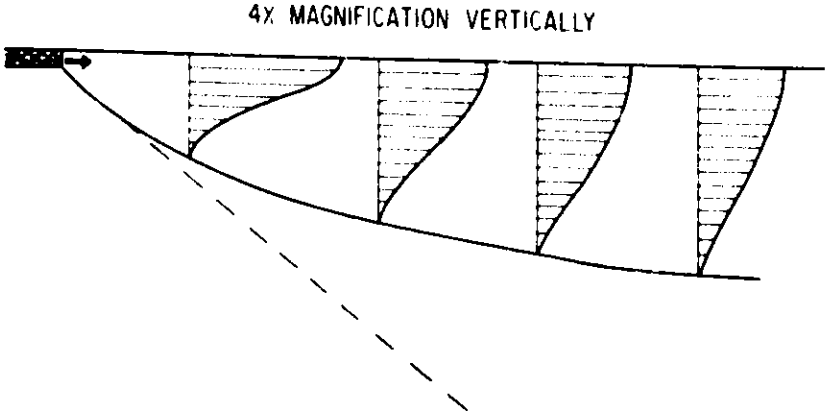

Fig. 6
Calculated Development of Mean Velocity Profiles in a Plane Surface Jet

An alternative way of viewing the effects of this stable stratification is through the reduction in the rate of entrainment of cool fluid into the jet. Ellison and Turner (1959) report experiments on the reduction in entrainment rates associated with a stable stratification. Figure 7 [Gibson and Launder (197?)] shows predictions of the fractional reduction in entrainment rate (relative to neutral flow) as a function of the degree of stratification; the quantity R_{i2}, defined by Ellison and Turner (1959), provides a dimensionless measure of the strength of the stratification. Evidently the experimentally measured entrainment rate is very sensitive to the level of R_{i2}, a sensitivity that is generally well reproduced by experiment.

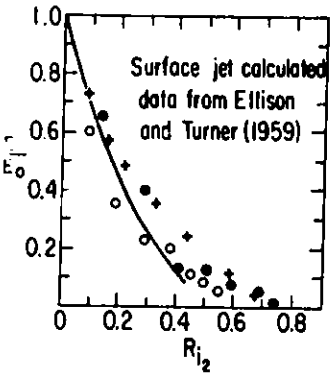

Fig. 7. Entrainment in Plane Surface Jet

The above example related to a horizontal flow. Hossain and Rodi (1977) have applied essentially the same model to calculate the rise of a vertical hot plume. Their work showed the need for a nonzero value of $c_{\epsilon 3}$ in Eq. 53. (Gibson and Launder had found their predictions to be only weakly dependent on $c_{\epsilon 3}$. Therefore, the inclusion of a nonzero $c_{\epsilon 3}$, which we now favor, would only slightly modify the Gibson-Launder results.)

Buoyant effects may also be of great importance in flows near walls; the earth's boundary layer is perhaps the most important example of a flow of this type. Experiments show, however, that there are striking differences in the nature of these effects, as compared to free flows. The differences have hitherto gone unnoticed or, at least, unreported, presumably because meteorologists are concerned only with the atmosphere, and civil engineers (whom local authorities traditionally turn to for solving problems of lake and river pollution) never get involved with "dry" fluids.

In terms of the present model, we can say that the cause of the difference may be traced to the near-wall correction to the pressure-strain and pressure-temperature gradient terms. Buoyancy greatly alters the distribution of length scale with distance from the wall (a stable stratification reducing the length scale at a given height above the surface). Now, the strength of the

wall correction is found to be roughly linearly dependent on the ratio of length scale to distance from the wall. (See Eq. 29, noting that $k^{3/2}/\varepsilon$ is an effective length scale of the energy-containing motions.) Thus, when ℓ decreases (as it does in a stable flow), the wall exerts a weaker effect than in neutral conditions. This is why, above a horizontal wall, there is apparently a slight increase in the fraction of turbulence energy contained in the vertical fluctuations as the stable stratification becomes progressivly stronger.

This behavior, which is contrary to that displayed in a free shear flow (and to what one's intuitions suggest), is well predicted by the model of Gibson and Launder (1978). Figure 8 shows predicted and measured variations of the ratio of vertical to streamwise velocity fluctuations under stable conditions. There is a good deal of scatter in the experimental data, which testifies to the difficulty of obtaining definitive turbulence data in the atmospheric boundary layer. The consensus of the experimental data suggests a rise of about 20% in $\sqrt{\overline{u_3^2}/\overline{u_1^2}}$ as the flux Richardson number, R_f, rises from zero to 0.1. (R_f represents the rate at which turbulence energy is destroyed by gravitational effects, divided by the rate at which it is created by mean shear; i.e., $R_f \equiv -G/P$.)

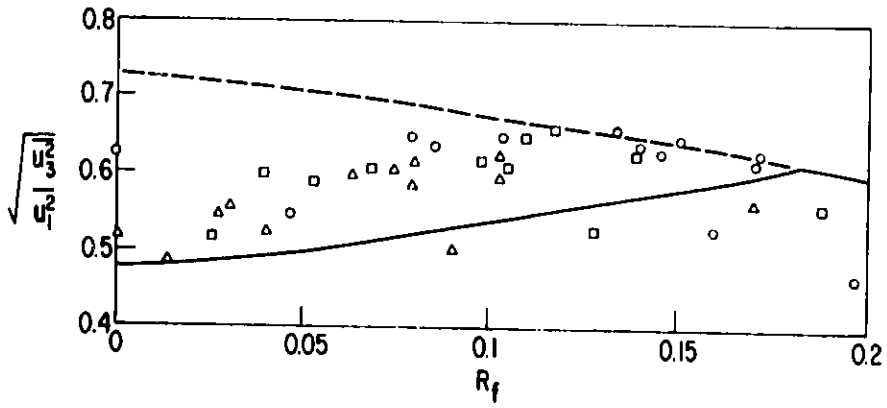

Fig. 8. Dependence of $\left(\overline{u_3^2}/\overline{u_1^2}\right)^{1/2}$ on Flux Richardson Number in Stably Stratified Flow. Atmospheric boundary-layer data from Haugan et al. (1971). Predictions: _____ wall flow; - - - - - - free shear flow.

The model predictions actually indicate that, for R_f greater than 0.18, the wall has no detectable effect in modifying the Reynolds stresses (because the effective length scale has become so small). That is why $\sqrt{\overline{u_3^2}/\overline{u_1^2}}$ starts to fall with further increase of R_f. In view of the scatter, it is hard to say from the data whether this feature is actually displayed; the predicted result is at least not inconsistent with the available measurements.

D. Three-dimensional Flows

Nearly all currently reported computations of three-dimensional heat transport have assumed the effective thermal diffusivity to be isotropic in the

plane normal to the mean velocity vector. Such isotropy, however, is by no means observed in practice. In an unsymmetrically heated pipe it is found that, near the wall, circumferential thermal diffusivities will be several times greater than radial ones. [See, for example, Black and Sparrow (1967) or Quarmby and Quirk (1972).] The present model does indeed produce a nonisotropic diffusion coefficient similar to what has been measured. The main cause of the higher circumferential diffusivity is (according to the present model) the greater intensity of velocity fluctuations in that direction.

As an illustration of the importance of this phenomenon, Fig. 9 relates to the spread of a jet of cool fluid discharged through a plate past which an external stream is flowing. It is part of an extensive film-cooling study by Bergeles et al. (1978). The figure shows the variation with distance downstream of the cooling effectiveness at the surface [$\eta \equiv (T_\infty - T_w)/(T_\infty - T_h)$, where the subscripts ∞, w, and h denote external-stream, wall, and hole-exit values, respectively]. Values are shown along the line passing through the hole center and at a representative off-centerline position. Two predicted curves are shown, one using a nonisotropic model similar to (though simpler than) that developed in the present work, and one in which the diffusivities were made isotropic. With the latter version, values of η along the centerline decay too slowly; off-center, the values remain too low. Using the nonisotropic model, however, entirely removes these shortcomings.

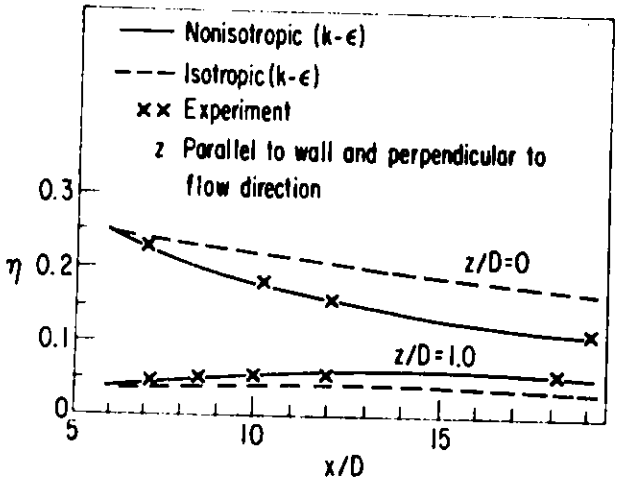

Fig. 9. Effect of Nonisotropic Transport Coefficients on Film-cooling Effectiveness

The final example considered is that of developing flow in noncircular ducts. The basic phenomenon of interest here is that, due to the inhomogeneity of the turbulence, weak mean-flow currents are established normal to the axis of the duct. These motions rarely exceed 1% of the mean flow, yet they may significantly modify the mean level of shear stress and heat-transfer coefficient and (more dramatically) the distribution of the local values of these quantities around the duct surface. Reece (1977) has computed the flow-field behavior for developing flow in a square-sectioned duct. His closure entailed the solution of transport equations for each of the stresses. Since, however, the flow develops only slowly in the streamwise direction, the use of the algebraic stress approximation, introduced in Sec. II.D, should not lead to significantly different results.

In fact, the most important aspect of the model for securing accurate predictions to this flow is the near-wall correction. Reece (1977) introduced the "linear-superposition" principle in treating the effects of the various walls of his duct, an idea that the present proposals have retained. Figure 10 compares the predicted mean flow contours with Melling's (1975) experiments at different positions from the duct entrance. Clearly evident is the progressive buildup of secondary motions along the duct, evidenced by the bulging of the axial velocity contours toward the corners. Agreement of the predictions with measurements is generally most satisfactory.

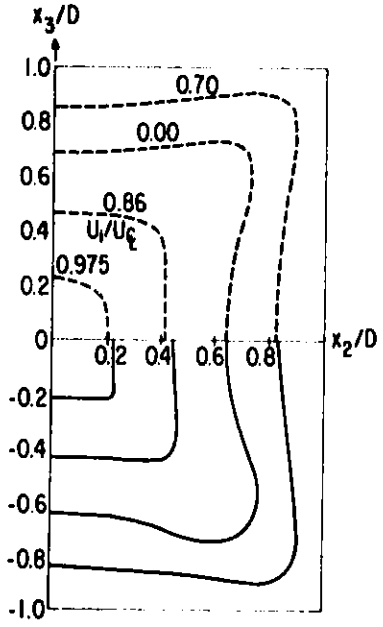

Fig. 10

Contours of Axial Mean Velocity in a Square Duct, at 29.0 Diameters from the Entrance. Data of Melling (1975) - - - - - ; predictions of Reece (1977) ———— .

V. CONCLUDING REMARKS

The present report has proposed a general closure for momentum and heat transport in turbulent flow for arbitrary Prandtl number. The aim has been to strike a balance between the competing requirements of complexity (to allow proper account to be taken of different processes affecting $\overline{u_i u_j}$ and $\overline{u_j \gamma}$) and economy (to keep the computer-core requirement as small as possible). In several respects, the detailed mathematical modeling of the physical processes needs further refinement or validation. Nevertheless, as the predictions of Sec. IV may have conveyed, the closure allows satisfactory prediction of several basic turbulence phenomena that would defeat simpler treatments.

APPENDIX A

The Turbulence-model Equations in Cartesian Coordinates

This appendix writes out, for a general three-dimensional flow using Cartesian coordinates, the turbulence-model equations developed in Sec. II. What follows presumes that the x_1 direction is vertically downward. Should the reader wish to treat the x_1 direction vertically upward, it merely requires a reversal of sign of the gravitational acceleration, denoted in this appendix as g_1.

The turbulence transport equations are presented first, followed by the algebraic Reynolds-stress and heat-flux equations.

The Turbulence-energy Equation

$$\frac{Dk}{Dt} = D_k + P + G - \epsilon. \tag{A.1}$$

The Energy-dissipation-rate Equation

$$\frac{D\epsilon}{Dt} = D_\epsilon + c_{\epsilon 1}\frac{(P+G)\epsilon}{k} - c_{\epsilon 2}\frac{\epsilon^2}{k}. \tag{A.2}$$

The Scalar Energy-transport Equation

$$\frac{Dg}{Dt} = D_g + P_g - \frac{\epsilon g}{kR} + \frac{\partial}{\partial x_1}\left(\frac{\lambda}{\rho c_p}\frac{\partial g}{\partial x_1}\right) + \frac{\partial}{\partial x_2}\left(\frac{\lambda}{\rho c_p}\frac{\partial g}{\partial x_2}\right) + \frac{\partial}{\partial x_3}\left(\frac{\lambda}{\rho c_p}\frac{\partial g}{\partial x_3}\right). \tag{A.3}$$

In the above,

$$\begin{aligned} D_\varphi \equiv\ & c_\varphi\left\{\frac{\partial}{\partial x_1}\left[\frac{k}{\epsilon}\left(\overline{u_1^2}\frac{\partial \varphi}{\partial x_1} + \overline{u_1u_2}\frac{\partial \varphi}{\partial x_2} + \overline{u_1u_3}\frac{\partial \varphi}{\partial x_3}\right)\right]\right. \\ & + \frac{\partial}{\partial x_2}\left[\frac{k}{\epsilon}\left(\overline{u_2u_1}\frac{\partial \varphi}{\partial x_1} + \overline{u_2^2}\frac{\partial \varphi}{\partial x_2} + \overline{u_2u_3}\frac{\partial \varphi}{\partial x_3}\right)\right] \\ & \left. + \frac{\partial}{\partial x_3}\left[\frac{k}{\epsilon}\left(\overline{u_3u_1}\frac{\partial \varphi}{\partial x_1} + \overline{u_3u_2}\frac{\partial \varphi}{\partial x_2} + \overline{u_3^2}\frac{\partial \varphi}{\partial x_3}\right)\right]\right\}, \end{aligned} \tag{A.4}$$

where φ stands for k, g, or ϵ.

$$\begin{aligned} P \equiv\ & -\left[\overline{u_1^2}\frac{\partial U_1}{\partial x_1} + \overline{u_1u_2}\left(\frac{\partial U_1}{\partial x_2} + \frac{\partial U_2}{\partial x_1}\right) + \overline{u_1u_3}\left(\frac{\partial U_1}{\partial x_3} + \frac{\partial U_3}{\partial x_1}\right)\right. \\ & \left. + \overline{u_2^2}\frac{\partial U_2}{\partial x_2} + \overline{u_2u_3}\left(\frac{\partial U_2}{\partial x_3} + \frac{\partial U_3}{\partial x_2}\right) + \overline{u_3^2}\frac{\partial U_3}{\partial x_3}\right]. \end{aligned} \tag{A.5}$$

$$P_g \equiv -\left(\overline{u_1\gamma}\frac{\partial\Gamma}{\partial x_1} + \overline{u_2\gamma}\frac{\partial\Gamma}{\partial x_2} + \overline{u_3\gamma}\frac{\partial\Gamma}{\partial x_3}\right). \tag{A.6}$$

$$G \equiv +\frac{\overline{\rho' u_1}}{\rho} g_1 = -\alpha\frac{\overline{u_1\gamma}}{\Gamma} g_1, \tag{A.7}$$

where α is the dimensionless volumetric expansion coefficient:

$$\alpha \equiv -\frac{\Gamma}{\rho}\frac{\partial\rho}{\partial\Gamma}\bigg|_p \tag{A.8}$$

The Reynolds Stress Equations

The following formulas do not provide detailed forms of the wall-correction term because these depend on the topography of the flow to be calculated.

$$\overline{u_1^2} = \frac{k}{\epsilon}\left(\frac{P+G}{\epsilon} + c_1 - 1\right)^{-1}\left\{(1-c_2)P_{11} + 2\left(1 - \tfrac{2}{3}c_3\right)G - \tfrac{2}{3}[\epsilon(1-c_1) - c_2 P] + \varphi_{11,w}\right\}, \tag{A.9}$$

where

$$P_{11} \equiv -2\left(\overline{u_1^2}\frac{\partial U_1}{\partial x_1} + \overline{u_1 u_2}\frac{\partial U_1}{\partial x_2} + \overline{u_1 u_3}\frac{\partial U_1}{\partial x_3}\right) \tag{A.10}$$

and

$$\overline{u_1 u_2} = \overline{u_2 u_1} = \frac{k}{\epsilon}\left(\frac{P+G}{\epsilon} + c_1 - 1\right)^{-1}[(1-c_2)P_{12} + (1-c_3)G_{12} + \varphi_{12,w}]; \tag{A.11}$$

where

$$P_{12} \equiv -\left(\overline{u_2 u_1}\frac{\partial U_1}{\partial x_1} + \overline{u_2^2}\frac{\partial U_1}{\partial x_2} + \overline{u_2 u_3}\frac{\partial U_1}{\partial x_3} + \overline{u_1^2}\frac{\partial U_2}{\partial x_1} + \overline{u_1 u_2}\frac{\partial U_2}{\partial x_2} + \overline{u_2 u_3}\frac{\partial U_2}{\partial x_3}\right), \tag{A.12}$$

$$G_{12} \equiv -\frac{\alpha u_2\gamma}{\Gamma} g_1, \tag{A.13}$$

and

$$\overline{u_1 u_3} = \overline{u_3 u_1} = \frac{k}{\epsilon}\left(\frac{P+G}{\epsilon} + c_1 - 1\right)^{-1}[(1-c_2)P_{13} + (1-c_2)G_{13} + \varphi_{13,w}]; \tag{A.14}$$

where

$$P_{13} \equiv -\left(\overline{u_3u_1}\frac{\partial U_1}{\partial x_1} + \overline{u_3u_2}\frac{\partial U_1}{\partial x_2} + \overline{u_3^2}\frac{\partial U_1}{\partial x_3} + \overline{u_1^2}\frac{\partial U_3}{\partial x_1} + \overline{u_1u_2}\frac{\partial U_3}{\partial x_2} + \overline{u_1u_3}\frac{\partial U_3}{\partial x_3}\right), \quad (A.15)$$

$$G_{13} \equiv -\frac{\alpha}{\Gamma}\overline{u_3\gamma}g_1, \quad (A.16)$$

and

$$\overline{u_2^2} = \frac{k}{\epsilon}\left(\frac{P+G}{\epsilon} + c_1 - 1\right)^{-1}\left\{(1-c_2)P_{22} + \tfrac{2}{3}[c_3G + c_2P - (1-c_1)\epsilon] + \varphi_{22,w}\right\}; \quad (A.17)$$

where

$$P_{22} = -2\left(\overline{u_2u_1}\frac{\partial U_2}{\partial x_1} + \overline{u_2^2}\frac{\partial U_2}{\partial x_2} + \overline{u_2u_3}\frac{\partial U_2}{\partial x_3}\right) \quad (A.18)$$

and

$$\overline{u_2u_3} = \overline{u_3u_2} = \frac{k}{\epsilon}\left(\frac{P+G}{\epsilon} + c_1 - 1\right)^{-1}[(1-c_2)P_{23} + \varphi_{23,w}]; \quad (A.19)$$

where

$$P_{23} \equiv -\left(\overline{u_2u_1}\frac{\partial U_3}{\partial x_1} + \overline{u_2^2}\frac{\partial U_3}{\partial x_2} + \overline{u_2u_3}\frac{\partial U_3}{\partial x_3} + \overline{u_3u_1}\frac{\partial U_2}{\partial x_1} + \overline{u_3u_2}\frac{\partial U_2}{\partial x_2} + \overline{u_3^2}\frac{\partial U_2}{\partial x_3}\right) \quad (A.20)$$

and

$$\overline{u_3^2} = \frac{k}{\epsilon}\left(\frac{P+G}{\epsilon} + c_1 - 1\right)^{-1}\left\{(1-c_2)P_{33} + \tfrac{2}{3}[c_2P + c_3G - (1-c_1)\epsilon] + \varphi_{33,w}\right\}; \quad (A.21)$$

where

$$P_{33} = -2\left(\overline{u_3u_1}\frac{\partial U_3}{\partial x_1} + \overline{u_3u_2}\frac{\partial U_3}{\partial x_2} + \overline{u_3^2}\frac{\partial U_3}{\partial x_3}\right). \quad (A.22)$$

The Velocity-Temperature Correlations

Note that the enthalpy fluxes are obtained from the velocity-temperature correlations by formulas of the type $\overline{-u_ih} = -c_p\overline{u_i\gamma}$.

As with the Reynolds stress equations, no explicit forms can be given for the wall correction.

$$\overline{u_1\gamma} = 2\left(\frac{P + G - \epsilon}{k} + \frac{P_g - \epsilon_g}{g} + \frac{c_{1\gamma}\epsilon}{kR^{1/2}}\right)^{-1}[\Gamma_{1\gamma} + (1 - c_{2\gamma})P_{1\gamma} + (1 - c_{3\gamma})G_{1\gamma} + \varphi_{1\gamma,w}], \tag{A.23}$$

where

$$\Gamma_{1\gamma} \equiv -\left(\overline{u_1^2}\frac{\partial\Gamma}{\partial x_1} + \overline{u_1u_2}\frac{\partial\Gamma}{\partial x_2} + \overline{u_1u_3}\frac{\partial\Gamma}{\partial x_3}\right), \tag{A.24}$$

$$P_{1\gamma} \equiv -\left(\overline{u_1\gamma}\frac{\partial U_1}{\partial x_1} + \overline{u_2\gamma}\frac{\partial U_1}{\partial x_2} + \overline{u_3\gamma}\frac{\partial U_1}{\partial x_3}\right), \tag{A.25}$$

$$G_{1\gamma} \equiv -2\alpha\frac{g}{\Gamma}g_1, \tag{A.26}$$

and

$$\overline{u_2\gamma} = 2\left(\frac{P + G - \epsilon}{k} + \frac{P_g - \epsilon_g}{g} + \frac{c_{1\gamma}\epsilon}{kR^{1/2}}\right)^{-1}[\Gamma_{2\gamma} + (1 - c_{2\gamma})P_{2\gamma} + \varphi_{2\gamma,w}]; \tag{A.27}$$

where

$$\Gamma_{2\gamma} \equiv -\left(\overline{u_1u_2}\frac{\partial\Gamma}{\partial x_1} + \overline{u_2^2}\frac{\partial\Gamma}{\partial x_2} + \overline{u_3u_2}\frac{\partial\Gamma}{\partial x_3}\right), \tag{A.28}$$

$$P_{2\gamma} = -\left(\overline{u_1\gamma}\frac{\partial U_2}{\partial x_1} + \overline{u_2\gamma}\frac{\partial U_2}{\partial x_2} + \overline{u_3\gamma}\frac{\partial U_2}{\partial x_3}\right), \tag{A.29}$$

and

$$u_3\gamma = 2\left(\frac{P + G - \epsilon}{k} + \frac{P_g - \epsilon_g}{g} + \frac{c_{1\gamma}\epsilon}{kR^{1/2}}\right)^{-1}[\Gamma_{3\gamma} + (1 - c_{2\gamma})P_{3\gamma} + \varphi_{3\gamma,w}]; \tag{A.30}$$

where

$$\Gamma_{3\gamma} \equiv -\left(\overline{u_1u_3}\frac{\partial\Gamma}{\partial x_1} + \overline{u_2u_3}\frac{\partial\Gamma}{\partial x_2} + \overline{u_3^2}\frac{\partial\Gamma}{\partial x_3}\right) \tag{A.31}$$

and

$$P_{3\gamma} \equiv -\left(\overline{u_1\gamma}\frac{\partial U_3}{\partial x_1} + \overline{u_2\gamma}\frac{\partial U_3}{\partial x_2} + \overline{u_3\gamma}\frac{\partial U_3}{\partial x_3}\right). \tag{A.32}$$

APPENDIX B

The Turbulence-model Equations in Cylindrical Polar Coordinates (r, θ, x)

The coordinates r and θ define horizontal planes, and the x coordinate is directly vertically downwards. Accordingly the gravitational acceleration is denoted as g_x.

1. Turbulence-energy Equation

$$\frac{\partial k}{\partial t} + U_r\frac{\partial k}{\partial r} + \frac{U_\theta}{r}\frac{\partial k}{\partial \theta} + U_x\frac{\partial k}{\partial x} = P + G - \epsilon + D_t(k) \qquad (B.1)$$

where

Generation rate due to mean shear,

$$P = \overline{u_r^2}\frac{\partial U_r}{\partial r} + \frac{\overline{u_r u_\theta}}{r}\frac{\partial U_r}{\partial \theta} + \overline{u_r u_x}\frac{\partial U_r}{\partial x} - \overline{u_r u_\theta}\frac{U_\theta}{r} + \overline{u_r u_\theta}\frac{\partial U_\theta}{\partial r} + \frac{\overline{u_\theta^2}}{r}\frac{\partial U_\theta}{\partial \theta}$$

$$+ \overline{u_\theta u_x}\frac{\partial U_\theta}{\partial x} + \overline{u_\theta^2}\frac{U_r}{r} + \overline{u_r u_x}\frac{\partial U_x}{\partial r} + \frac{\overline{u_\theta u_x}}{r}\frac{\partial U_x}{\partial \theta} + \overline{u_x^2}\frac{\partial U_x}{\partial x}, \qquad (B.2)$$

Generation rate due to buoyant interaction,

$$G = \frac{\overline{\rho' u_x}}{\rho} g_x \qquad (B.3)$$

with the temperature-density relationship

$$G = -\frac{\alpha}{\Gamma}\overline{\gamma u_x} g_x, \qquad (B.4)$$

Turbulent diffusion of turbulent kinetic energy,

$$D_t(k) = c_s\frac{1}{r}\frac{\partial}{\partial r}\left(\frac{rk\overline{u_r^2}}{\epsilon}\frac{\partial k}{\partial r}\right) + c_s\frac{1}{r}\frac{\partial}{\partial r}\left(r\frac{k}{\epsilon}\overline{u_r u_\theta}\frac{\partial k}{r\partial \theta}\right) + c_s\frac{1}{r}\frac{\partial}{\partial r}\left(r\frac{k}{\epsilon}\overline{u_r u_x}\frac{\partial k}{\partial x}\right)$$

$$+ c_s\frac{\partial}{r\partial \theta}\left(\frac{k}{\epsilon}\overline{u_r u_\theta}\frac{\partial k}{\partial r}\right) + c_s\frac{\partial}{r\partial \theta}\left(\frac{k}{\epsilon}\overline{u_\theta^2}\frac{\partial k}{r\partial \theta}\right) + c_s\frac{\partial}{r\partial \theta}\left(\frac{k}{\epsilon}\overline{u_\theta u_x}\frac{\partial k}{\partial x}\right)$$

$$+ c_s\frac{\partial}{\partial x}\left(\frac{k}{\epsilon}\overline{u_r u_x}\frac{\partial k}{\partial r}\right) + c_s\frac{\partial}{\partial x}\left(\frac{k}{\epsilon}\overline{u_\theta u_x}\frac{\partial k}{r\partial \theta}\right) + c_s\frac{\partial}{\partial x}\left(\frac{k}{\epsilon}\overline{u_x^2}\frac{\partial k}{\partial x}\right) \qquad (B.5)$$

2. The Energy-dissipation-rate Equation

$$\frac{\partial \epsilon}{\partial t} + U_r\frac{\partial \epsilon}{\partial r} + U_\theta\frac{\partial \epsilon}{r\partial\theta} + U_x\frac{\partial \epsilon}{\partial x} = c_{\epsilon 1}\frac{\epsilon}{k}P + c_{\epsilon 3}\frac{\epsilon}{k}G - c_{\epsilon 2}\frac{\epsilon^2}{k} + D(\epsilon) \qquad (B.6)$$

The generation rates P and G were given earlier.

Diffusion rate of dissipation,

$$D(\epsilon) = c_\epsilon\frac{1}{r}\frac{\partial}{\partial r}\left(r\frac{k}{\epsilon}\overline{u_r^2}\frac{\partial \epsilon}{\partial r}\right) + c_\epsilon\frac{1}{r}\frac{\partial}{\partial r}\left(r\frac{k}{\epsilon}\overline{u_r u_\theta}\frac{\partial \epsilon}{r\partial\theta}\right) + c_\epsilon\frac{1}{r}\frac{\partial}{\partial r}\left(r\frac{k}{\epsilon}\overline{u_r u_x}\frac{\partial \epsilon}{\partial x}\right)$$

$$+ c_\epsilon\frac{\partial}{r\partial\theta}\left(\frac{k}{\epsilon}\overline{u_r u_\theta}\frac{\partial \epsilon}{\partial r}\right) + c_\epsilon\frac{\partial}{r\partial\theta}\left(\frac{k}{\epsilon}\overline{u^2}\frac{\partial \epsilon}{r\partial\theta}\right) + c_\epsilon\frac{\partial}{r\partial\theta}\left(\frac{k}{\epsilon}\overline{u_\theta u_x}\frac{\partial \epsilon}{\partial x}\right)$$

$$+ c_\epsilon\frac{\partial}{\partial x}\left(\frac{k}{\epsilon}\overline{u_r u_x}\frac{\partial \epsilon}{\partial r}\right) + c_\epsilon\frac{\partial}{\partial x}\left(\frac{k}{\epsilon}\overline{u_\theta u_x}\frac{\partial g}{r\partial\theta}\right) + c_\epsilon\frac{\partial}{\partial x_1}\left(\frac{k}{\epsilon}\overline{u_x^2}\frac{\partial \epsilon}{\partial x}\right). \qquad (B.7)$$

3. The Scalar-energy-transport Equation

$$\frac{\partial g}{\partial t} + U_r\frac{\partial g}{\partial r} + U_\theta\frac{\partial g}{r\partial\theta} + U_x\frac{\partial g}{\partial x} = P_g - \frac{\epsilon g}{kR} + D_t(g) + D_m(g) \qquad (B.8)$$

Generation rate of temperature fluctuation,

$$P_g = -\overline{u_r\gamma}\frac{\partial \Gamma}{\partial r} - \overline{u_\theta\gamma}\frac{\partial \Gamma}{r\partial\theta} - \overline{u_x\gamma}\frac{\partial \Gamma}{\partial x} \qquad (B.9)$$

Turbulent diffusion rate of g,

$$D_t(g) = c_g\frac{1}{r}\frac{\partial}{\partial r}\left(r\frac{k}{\epsilon}R^{1/2}\overline{u_r^2}\frac{\partial g}{\partial r}\right) + c_g\frac{1}{r}\frac{\partial}{\partial r}\left(r\frac{k}{\epsilon}R^{1/2}\overline{u_r u_\theta}\frac{\partial g}{r\partial\theta}\right)$$

$$+ c_g\frac{1}{r}\frac{\partial}{\partial r}\left(r\frac{k}{\epsilon}R^{1/2}\overline{u_r u_x}\frac{\partial g}{\partial x}\right) + c_g\frac{\partial}{r\partial\theta}\left(\frac{k}{\epsilon}R^{1/2}\overline{u_r u_\theta}\frac{\partial g}{\partial r}\right)$$

$$+ c_g\frac{\partial}{r\partial\theta}\left(\frac{k}{\epsilon}R^{1/2}\overline{u_\theta^2}\frac{\partial g}{r\partial\theta}\right) + c_g\frac{\partial}{r\partial\theta}\left(\frac{kR^{1/2}}{\epsilon}\overline{u_\theta u_x}\frac{\partial g}{\partial x}\right)$$

$$+ c_g\frac{\partial}{\partial x}\left(\frac{k}{\epsilon}R^{1/2}\overline{u_r u_x}\frac{\partial g}{\partial r}\right) + c_g\frac{\partial}{\partial x}\left(\frac{kR^{1/2}}{\epsilon}\overline{u_\theta u_x}\frac{\partial g}{r\partial\theta}\right)$$

$$+ c_g\frac{\partial}{\partial x}\left(\frac{k}{\epsilon}R^{1/2}\overline{u_x^2}\frac{\partial g}{\partial x}\right) \qquad (B.10)$$

Molecular diffusion rate of g,

$$D_m(g) = \frac{1}{\rho}\left[\frac{1}{r}\frac{\partial}{\partial r}\left(\frac{r\lambda}{c_p}\frac{\partial g}{\partial r}\right) + \frac{1}{r}\frac{\partial}{\partial r}\left(\frac{r\lambda}{c_p}\frac{\partial g}{r\partial\theta}\right) + \frac{1}{r}\frac{\partial}{\partial r}\left(\frac{r\lambda}{c_p}\frac{\partial g}{\partial x}\right)\right.$$

$$+ \frac{\partial}{r\partial\theta}\left(\frac{\lambda}{c_p}\frac{\partial g}{\partial r}\right) + \frac{\partial}{r\partial\theta}\left(\frac{\lambda}{c_p}\frac{\partial g}{r\partial\theta}\right) + \frac{\partial}{r\partial\theta}\left(\frac{\lambda}{c_p}\frac{\partial g}{\partial x}\right)$$

$$\left. + \frac{\partial}{\partial x}\left(\frac{\lambda}{c_p}\frac{\partial g}{r\partial\theta}\right) + \frac{\partial}{\partial x}\left(\frac{\lambda}{c_p}\frac{\partial g}{\partial x}\right)\right] \qquad (B.11)$$

The Reynolds stress equations and velocity-temperature correlations used above are defined below.

4. The Reynolds Stress Equations

$$\overline{u}_r^2 = \frac{k}{\epsilon}\left[(c_1 - 1) + \frac{P + G}{\epsilon}\right]^{-1}\left[-\left(2\overline{u}_r^2\frac{\partial U_r}{\partial r} + 2\overline{u_r u_\theta}\frac{\partial U_r}{r\partial\theta} + 2\overline{u_r u_x}\frac{\partial U_r}{\partial x}\right.\right.$$

$$\left. - 2\overline{u_r u_\theta}\frac{U_\theta}{r}\right) - c_2\left[-\left(2\overline{u}_r^2\frac{\partial U_r}{\partial r} + 2\overline{u_r u_\theta}\frac{\partial U_r}{r\partial\theta} + 2\overline{u_r u_x}\frac{\partial U_r}{\partial x} - 2\overline{u_r u_\theta}\frac{U_\theta}{r}\right) - \tfrac{2}{3}P\right]$$

$$\left. - C_3\left(-\tfrac{2}{3}G\right) + \varphi_{rr,w} + \tfrac{2}{3}(c_1 - 1)\epsilon\right], \qquad (B.12)$$

$$\overline{u}_\theta^2 = \frac{k}{\epsilon}\left[(c_1 - 1) + \frac{P + G}{\epsilon}\right]^{-1}\left[-\left(2\overline{u_\theta u_r}\frac{\partial U_\theta}{\partial r} + 2\overline{u}_\theta^2\frac{\partial U_\theta}{r\partial\theta} + 2\overline{u_\theta u_x}\frac{\partial U_\theta}{\partial x}\right.\right.$$

$$\left. + 2\overline{u}_\theta^2\frac{U_r}{r}\right) - c_2\left[-\left(2\overline{u_\theta u_r}\frac{\partial U_\theta}{\partial r} + 2\overline{u}_\theta^2\frac{\partial U_\theta}{r\partial\theta} + 2\overline{u_\theta u_x}\frac{\partial U_\theta}{\partial x}\right.\right.$$

$$\left.\left. + 2\overline{u}_\theta^2\frac{U_r}{r}\right) - \tfrac{2}{3}P\right] - c_3\left(-\tfrac{2}{3}G\right) + \varphi_{\theta\theta,w} + \tfrac{2}{3}(c_1 - 1)\epsilon\right], \qquad (B.13)$$

$$\overline{u}_x^2 = \frac{k}{\epsilon}\left[(c_1 - 1) + \frac{P + G}{\epsilon}\right]^{-1}\left[-\left(2\overline{u_x u_r}\frac{\partial U_x}{\partial r} + 2\overline{u_x u_\theta}\frac{\partial U_x}{r\partial\theta} + 2\overline{u_x u_x}\frac{\partial U_x}{\partial x}\right)\right.$$

$$-\left(\frac{2\alpha}{\Gamma}\overline{\gamma u}_x g_x\right) - C_2\left[-\left(2\overline{u_x u_r}\frac{\partial U_x}{\partial r} + 2\overline{u_x u_\theta}\frac{\partial U_x}{r\partial\theta} + 2\overline{u_x u_x}\frac{\partial U_x}{\partial x}\right) - \tfrac{2}{3}P\right]$$

$$\left. - C_3\left(-\frac{2\alpha}{\Gamma}\overline{\gamma u}_x g_x - \tfrac{2}{3}G\right) + \varphi_{xx,w} + \tfrac{2}{3}(c_1 \quad 1)\epsilon\right], \qquad (B.14)$$

$$\overline{u_r u_\theta} = \frac{k}{\epsilon}\left[(c_1 - 1) + \frac{P + G}{\epsilon}\right]^{-1}\left[-\left(\overline{u_r^2}\frac{\partial U_\theta}{\partial r} + \overline{u_r u_\theta}\frac{\partial U_\theta}{r\partial\theta} + \overline{u_r u_\theta}\frac{U_r}{r} + \overline{u_r u_x}\frac{\partial U_\theta}{\partial x}\right.\right.$$

$$\left.\left. + \overline{u_\theta u_r}\frac{\partial U_r}{\partial r} + \overline{u_\theta^2}\frac{\partial U_r}{r\partial\theta} - \overline{u_\theta^2}\frac{U_\theta}{r} + \overline{u_\theta u_x}\frac{\partial U_r}{\partial x}\right)(1 - c_2) + \varphi_{r\theta,w}\right], \qquad \text{(B.15)}$$

$$\overline{u_r u_x} = \frac{k}{\epsilon}\left[(c_1 - 1) + \frac{P + G}{\epsilon}\right]^{-1}\left[-\left(\overline{u_r^2}\frac{\partial U_x}{\partial r} + \overline{u_r u_\theta}\frac{\partial U_x}{r\partial\theta} + \overline{u_r u_x}\frac{\partial U_x}{\partial x} + \overline{u_x u_r}\frac{\partial U_r}{\partial r}\right.\right.$$

$$\left.\left. + \overline{u_x u_\theta}\frac{\partial U_r}{r\partial\theta} + \overline{u_x^2}\frac{\partial U_r}{\partial x} - \overline{u_x u_\theta}\frac{U_\theta}{r}\right)(1 - c_2) - \left(\frac{\alpha}{\Gamma}\overline{\gamma u_r}g_x\right)(1 - c_3) + \varphi_{rx,w}\right], \qquad \text{(B.16)}$$

and

$$\overline{u_\theta u_x} = \frac{k}{\epsilon}\left[(c_1 - 1) + \frac{P + G}{\epsilon}\right]^{-1}\left[-\left(\overline{u_\theta u_r}\frac{\partial U_x}{\partial r} + \overline{u_\theta^2}\frac{\partial U_x}{r\partial\theta} + \overline{u_\theta u_x}\frac{\partial U_x}{\partial x} + \overline{u_x u_r}\frac{\partial U_\theta}{\partial r}\right.\right.$$

$$\left.\left. + \overline{u_x u_\theta}\frac{\partial U_\theta}{r\partial\theta} + \overline{u_x^2}\frac{\partial U_\theta}{\partial x} + \overline{u_x u_\theta}\frac{U_r}{r}\right)(1 - c_2)\ \left(\frac{\alpha}{\Gamma}\overline{\gamma u_\theta}g_x\right)(1 - c_3) + \varphi_{\theta x,w}\right]. \qquad \text{(B.17)}$$

5. The Velocity-Temperature Correlations

$$\overline{u_r\gamma} = 2\left[\frac{P_g}{g} + \frac{P + G}{k} - \frac{\epsilon}{k}\left(1 + \frac{1}{R} - c_{1\gamma}F_1(Pe)\right)\right]^{-1}\left[-\left(\overline{u_r^2}\frac{\partial\Gamma}{\partial r} + \overline{u_r u_\theta}\frac{\partial\Gamma}{r\partial\theta} + \overline{u_r u_x}\frac{\partial\Gamma}{\partial x}\right)\right.$$

$$\left. - \left(\overline{u_r\gamma}\frac{\partial U_r}{\partial r} + \overline{u_\theta\gamma}\frac{\partial U_r}{r\partial\theta} + \overline{u_x\gamma}\frac{\partial U_r}{\partial x} - \overline{u_\theta\gamma}\frac{U_\theta}{r}\right)(1 - c_{2\gamma}) + \varphi_{r\gamma,w}\right], \qquad \text{(B.18)}$$

$$\overline{u_\theta\gamma} = 2\left[\frac{P_g}{g} + \frac{P + G}{k} - \frac{\epsilon}{k}\left(1 + \frac{1}{R} - c_{1\gamma}F_1(Pe)\right)\right]^{-1}\left[-\left(\overline{u_r u_\theta}\frac{\partial\Gamma}{\partial r} + \overline{u_\theta^2}\frac{\partial\Gamma}{r\partial\theta} + \overline{u_\theta u_x}\frac{\partial\Gamma}{\partial x}\right)\right.$$

$$\left. - \left(\overline{u_r\gamma}\frac{\partial U_\theta}{\partial r} + \overline{u_\theta r}\frac{\partial U_\theta}{r\partial\theta} + \overline{u_x\gamma}\frac{\partial U_\theta}{\partial x} + \overline{u_\theta\gamma}\frac{U_r}{r}\right)(1 - c_{2\gamma}) + \varphi_{\theta\gamma,w}\right], \qquad \text{(B.19)}$$

and

$$\overline{u_x\gamma} = 2\left[\frac{P_g}{g} + \frac{P + G}{k} - \frac{\epsilon}{k}\left(1 + \frac{1}{R} - c_{1\gamma}F_1(Pe)\right)\right]^{-1}\left[-\left(\overline{u_r u_x}\frac{\partial\Gamma}{\partial r} + \overline{u_\theta u_x}\frac{\partial\Gamma}{r\partial\theta} + \overline{u_x^2}\frac{\partial\Gamma}{\partial x}\right)\right.$$

$$\left. - \left(\overline{u_r\gamma}\frac{\partial U_x}{\partial r} + \overline{u_\theta\gamma}\frac{\partial U_x}{r\partial\theta} + \overline{u_x\gamma}\frac{\partial U_x}{\partial r}\right)(1 - c_{2\gamma}) - \left(\frac{\alpha}{\Gamma}\overline{\gamma}^2 g_x\right)(1 - c_{3\gamma}) + \varphi_{x,\gamma,w}\right]. \qquad \text{(B.20)}$$

APPENDIX C

Systematic Simplifications of Proposed Turbulence Model

The simplifications proposed in this appendix are arranged so that they may be applied sequentially. That is, the first proposal implies that least modification; the second proposal used in conjunction with the first represents a further simplification, and so on.

Simplification 1: Elimination of Transport Equation for Mean-square Temperature Variance, g

The transport equation for g is replaced by the simple algebraic formula that results from equating generation and production agencies in Eq. 52 of the main text.

$$0 = P_g - \frac{\epsilon g}{kR}$$

or

$$g = P_g kR/\epsilon, \tag{C.1}$$

where

$$P_g = -\overline{u_{k\gamma}}\partial\Gamma/\partial x_k$$

and R may be obtained from Eq. 54:

$$R = 0.7[1 - \exp(-Pe_t/a')]^2. \tag{C.2}$$

To save computational time, Eq. C.2 could be replaced by its high-Peclet-number asymptote R = 0.7.

In connection with this simplification, consistent assumptions need to be introduced into the heat-flux formula, Eq. 50, since g appears there in the denominator and could thus cause instabilities when P_g becomes very small. The first group of terms in braces of Eq. 50 should thus read

$$\overline{u_j\gamma} = 2\left\{\frac{(P + G)}{k} + \frac{\epsilon}{k}[2c_{1\gamma}F_1(Pe_t) - 1]\right\}^{-1}\left[-\overline{u_j u_k}\frac{\partial\Gamma}{\partial x_k} + \ldots\right]. \tag{C.3}$$

Correspondingly, the group $(P_g - \epsilon_g)/g$ in Eqs. A.23 and A.27 should be dropped, as should likewise the same terms in Eqs. B.18-B.20. (Due to a slightly different algebraic presentation, the terms P_g/g and $-\epsilon/Rk$ in the first brackets on the right need to be suppressed.)

Experience gained by Professor Launder's group and that of Dr. W. Rodi of the SFB80 of the University of Karlsruhe suggests that the above simplifications will usually not produce significantly different calculated behavior from that given by the complete model.

Simplification 2: Replacement of Algebraic Stress Closure by Isotropic-turbulent-viscosity Approach Based on Solution of the k and ε Equations

This approach eliminates most of the auxiliary algebra coupling the stresses and heat fluxes to one another. Buoyant influences can be included in only very rough ways, but this may suffice for initial testing.

In place of Eqs. 49 and 50, the following equations should be inserted:

$$\overline{u_i u_j} = \tfrac{2}{3} k \delta_{ij} - c_\nu \frac{k^2}{\varepsilon}\left(\frac{\partial U_i}{\partial x_j} + \frac{\partial U_j}{\partial x_i}\right) \tag{C.4}$$

and

$$\overline{u_j \gamma} = \frac{\nu_t}{\sigma_t} \frac{\partial \Gamma}{\partial x_j}, \tag{C.5}$$

where

$$\left.\begin{aligned} c_\nu &= 0.09(1 - 3.0G/P) \\ \text{or} \\ c_\nu &= 0 \end{aligned}\right\} \text{whichever is greater} \tag{C.6}$$

and

$$\sigma_t = 0.9/[1 - \exp(-Pe_t/a')]. \tag{C.7}$$

Equation C.6 eliminates turbulent shear stresses whenever the local flux Richardson number exceeds 1/3; Eq. C.7 puts in the dependence of turbulent Prandtl number on turbulent Peclet number that is indicated by Eq. 54 of the main text under local-equilibrium conditions.

When buoyant effects are negligible, this approach has proved to be competitive in accuracy with the more complete formulation proposed in the main report.

Simplification 3: Elimination of Transport Equation for Dissipation Rate

The following rather drastic simplification may be justified for internal flows if recirculation is absent or of very limited extent and turbulent flow extends over the whole region, for example, in flow through a pipe not too close to the entrance.

The transport equation for ϵ is replaced by the formula

$$\epsilon = k^{3/2}/\ell, \tag{C.8}$$

where the length scale ℓ is taken as the smaller of

$\ell = 2.5x_n$, x_n being the distance to the nearest wall,

or

$\ell = 0.6d_h$, d_h being the hydraulic diameter of the containing vessel.

For flow through pipe-like containers the hydraulic diameter should be obtained from the conventional definition (i.e., d_h = 4 x cross-section area/wetted perimeter). For motions in a tank, it may be more appropriate to take

d_h = 6 x volume/surface area.

The above proportionality constant was chosen so that, for a spherical container, the hydraulic diameter exactly equals the actual diameter of the sphere.

It needs to be emphasized that in complex recirculating flows the above suggestions will provide only a very rough guide to the level of the turbulent stresses.

Simplification 4: Elimination of Transport Equation for Turbulence Energy

For local equilibrium in a simple shear flow, the equality of turbulence energy generation and dissipation rates implies

$$-\overline{uv}\frac{\partial U}{\partial y} = \frac{k^{3/2}}{\ell} \tag{C.9}$$

and

$$-\overline{uv} = 0.3k.$$

Hence by eliminating $\overline{uv}$, we obtain

$$k^{1/2} = 0.3\ell\frac{\partial U}{\partial y}. \tag{C.10}$$

The use of this formula eliminates the need to solve Eq. 51. The resultant turbulence model is essentially Prandtl's mixing-length hypothesis ($m\ell h$). To generalize Eq. C.10 to situations in which there are several nonzero components of the velocity gradient or, equally, to regions in which all mean strain is zero or very small, we propose the following form:

$$\left.\begin{aligned} k &= 0.09\ell^2\left(\frac{\partial U_i}{\partial x_j}\right)^2 \\ \text{or} \\ k &= 5 \times 10^{-4}\overline{U}^2, \end{aligned}\right\} \tag{C.11}$$

whichever is larger, where $\overline{U}$ represents some characteristic average velocity through the vessel.

The above scheme is probably of nearly the same width of validity as Simplification 3, i.e., it is useful for near-equilibrium external flows without recirculation.

ACKNOWLEDGMENTS

We acknowledge Drs. S. M. Cho, H. L. Chou, and T. T. Kao of Foster Wheeler Energy Corporation, J. J. Oras and C. I. Yang of Argonne National Laboratory, and C. E. Ockert of RRT, Department of Energy, for their comments and suggestions.

REFERENCES

J. Andre et al., *Une Approche Statistique de la Turbulence Inhomogine*, Thèse Docteur ès Sciences, Université Pierre et Marie Curie, Paris (1976).

C. Beguier, I. Dekeyser, and B. E. Launder, *On the Ratio of Scalar and Velocity Dissipation Time Scales in Shear Flow Turbulence*, J. Fluid Mech. *21*, 307-310 (1978).

G. Bergeles, A. D. Gosman, and B. E. Launder, *The Turbulent Jet in a Cross-Stream at Low Injection Rates: A Three-Dimensional Numerical Treatment*, Numerical Heat Transfer *1*(2), 217-242 (1978).

A. W. Black and E. M. Sparrow, *Experiments on Turbulent Heat Transfer in a Tube with Circumferentially Varying Thermal Boundary Conditions*, J. Heat Transfer *89*, 258-268 (1967).

P. Y. Chou, *On Velocity Correlations and the Solutions of the Equations of Turbulent Fluctuations*, Q. J. Mech. Appl. Math. *3*, 38-54 (1945).

S. C. Corrsin, *Heat Transfer in Isotropic Turbulence*, J. Appl. Phys. *23*, 113-118 (1952).

B. J. Daly and F. H. Harlow, *Transport Equations in Turbulence*, Phys. Fluids *13*, 2634-2649 (1970).

R. G. Deissler, *Turbulent Heat Transfer and Temperature Fluctuations in a Field with Uniform Velocity and Temperature Gradients*, Int. J. Heat Mass Transfer *6*, 257-270 (1963).

C. duP. Donaldson, *A Computer Study of an Analytical Model of Boundary Layer Transition*, AIAA Paper No. 68-38 (1968).

C. duP. Donaldson, R. D. Sullivan, and H. Rosenbaum, *Calculation of Turbulent Shear Flows for Atmospheric and Vortex Motions*, AIAA J. *10*, 4-12 (1972).

T. H. Ellison and J. S. Turner, *Turbulent Entrainment in Stratified Flows*, J. Fluid Mech. *6*, 423-448 (1959).

M. M. Gibson and B. E. Launder, *On the Calculation of Horizontal, Turbulent, Free Shear Flows Under Gravitational Influence*, J. Heat Transfer *98*, 81-87 (1976).

M. M. Gibson and B. E. Launder, *Ground Effects on Pressure Fluctuations in the Atmospheric Boundary Layer*, J. Fluid Mech. *86*, 491-511 (1978).

K. Hanjalić and B. E. Launder, *A Reynolds Stress Model of Turbulence and Its Application to Thin Shear Flows*, J. Fluid Mech. *52*, 609-638 (1972).

D. A. Haugan, J. C. Kaimal, and E. F. Bradley, *An Experimental Study of Reynolds Stress and Heat Flux in the Atmospheric Surface Layer*, Q. J. R. Meteor. Soc. *97*, 168-180 (1970).

M. S. Hossain and W. Rodi, "Influence of Buoyancy on the Turbulence Intensities in Horizontal and Vertical Jets," *Heat Transfer and Turbulent Buoyant Convection*, D. Brian Spalding and N. Afgan, eds., pp. 39-51 (1977).

F. J. K. Ideriah, private communication (1976).

H. P. A. H. Irwin, *Measurements in Blown Boundary Layers and Their Prediction by Reynolds Stress Modelling*, Ph.D. thesis, McGill University, Montreal, Canada (1974).

C. L. V. Jayatilleke, *The Influence of Prandtl Number and Surface Roughness on the Resistance of the Laminar Sub-Layer to Momentum and Heat Transfer*, Prog. Heat Mass Transfer *1*, 193-329 (1967).

P. E. Jenkins and V. W. Goldschmidt, *Mean Temperature and Velocity in a Plane Turbulent Jet*, J. Fluids Eng. *95*, 581-584 (1973).

W. P. Jones and B. E. Launder, *The Prediction of Laminarization with a Two-Equation Model of Turbulence*, Int. J. Heat Mass Transfer *15*, 301-314 (1972).

A. N. Kolmogorov, *Equations of Turbulent Motion of an Incompressible Turbulent Fluid*, Izv. Akad. Nauk SSSR, Ser. Fiz. *VI* (1-2), 56 (1942).

B. Kolovandin "Asymptotic Correlational Modeling of Inhomogeneous Turbulence," *Proc. Symp. Turbulent Shear Flows*, Penn State University, University Park, Pa., Vol. 1, Paper 17D, pp. 17.23-17.30 (Apr 18-20, 1977).

B. E. Launder, *An Improved Algebraic Modeling of the Reynolds Stresses*, Imperial College, London, Engineering Department Report TM-TN-A9 (1971).

B. E. Launder et al., "Prediction of Free Shear Flows--A Comparison of the Performance of Six Turbulence Models," *Proc. Free Turbulent Shear Flows Conf.*, NASA Langley Research Center, NASA SP 321 1973, pp. 361-426 (July 20-21, 1972).

B. E. Launder, *On the Effects of a Gravitational Field on the Turbulent Transport of Heat and Momentum*, J. Fluid Mech. *67*, 569-581 (1975A).

B. E. Launder, *Progress in the Modelling of Turbulent Transport*, Lecture Series No. 76, von Karman Inst., Belgium (1975B).

B. E. Launder, "Heat and Mass Transport," *Turbulence*, P. Bradshaw, ed., Vol. 12: *Topics in Applied Physics*, Chap. 6, pp. 232-287, Springer, Berlin (1976).

B. E. Launder, G. J. Reece, and W. Rodi, *Progress in the Development of a Reynolds-Stress Turbulence Closure*, J. Fluid Mech. *68*, 537-566 (1975).

B. E. Launder and D. B. Spalding, *The Numerical Computation of Turbulent Flows*, Comput. Methods Appl. Mech. Eng. *3*, 269-289 (1974).

B. E. Launder and W. M. Ying, "Prediction of Flow and Heat Transfer in Ducts of Square Cross Section," *Proc. Inst. Mech. Eng.*, London, Vol. 187, Paper No. 37, pp. 454-461 (1973).

C. J. Lawn, *Turbulent Temperature Fluctuations in Liquid Metals*, Int. Heat Mass Transfer *20*, 1035-1044 (1977).

J. L. Lumley, "A Model for Computation of Stratified Turbulent Flows," *Proc. Int. Symp. on Stratified Flow*, Novosibirsk, USSR (1972).

J. L. Lumley and B. J. Khajeh-Nouri, *Computational Modeling of Turbulent Transport*, Adv. Geophys. *18A*, 169-192 (1974).

J. L. Lumley, *Prediction Methods for Turbulent Flow; Introduction*, Lecture Series No. 76, von Karman Inst., Belgium (1975).

A. Melling, *Investigation of Flow in Non-Circular Ducts and Other Configurations by Laser Doppler Anemometry*, Ph.D. thesis, Faculty of Mech. Eng., University of London (1975).

G. L. Mellor, *Analytical Prediction of the Properties of Stratified Planetary Surface Layers*, J. Atmos. Sci. *30*, 1061-1069 (1973).

NASA, *Proceedings of the Free Shear Flow Conference* (1973).

R. G. Owen, *An Analytical Turbulent Transport Model Applied to Non-Isothermal Fully Developed Duct Flows*, Ph.D. thesis, Mech. Eng. Dept., Penn State University (1973).

L. Prandtl, *Bericht über Untersuchungen zur Ausgebildeten Turbulenz*, Z. Angew. Math. Mech. *5*, 136 (1925).

L. Prandtl and K. Wieghardt, *Uber ein neues Formelsystem fur die Ausgebildete Turbulenz*, Nachr. Akad. Wiss., Gottingen, Math.-Phys. Kl., 6-19 (1945).

A. Quarmby and R. Quirk, *Measurements of the Radial and Tangential Eddy Diffusivities of Heat and Mass in Turbulent Flow in a Plain Tube*, Int. J. Heat Mass Transfer *15*, 2309-2327 (1972).

G. J. Reece, *Development and Application of a Generalized Reynolds Stress Model of Turbulence*, Ph.D. thesis, University of London (1977).

W. Rodi, *The Prediction of Free Turbulent Boundary Layers by Use of a 2-Equation Model of Turbulence*, Ph.D. thesis, Faculty of Mech. Eng., University of London (1972).

J. C. Rotta, *Statistische Theorie Nichthomogener Turbulenz*, Z. Physik *129*, 547-572 (1951).

D. S. A. Samaraweera, *Turbulent Heat Transport in Two- and Three- Dimensional Temperature Fields*, Ph.D. thesis, Faculty of Engineering, University of London (1978).

J. Siess, *Etude d'après la Methode de J. Lumley de la Penetration de la Turbulence dans un Milieu Stratifié*, Thèse Dr. Ing, Université d'Aix Marseille (1975).

F. Tamanini, *Algebraic Stress Modeling in a Buoyancy Controlled Turbulent Shear Flow*, Paper 6D, pp. 6.29-6.38 (1975).

G. I. Taylor, *Eddy Motion in the Atmosphere*, Phil. Trans. R. Soc. London, Ser. A *215*, 1-26, (1915).

H. Tennekes and J. L. Lumley, *A First Course in Turbulence*, MIT Press, Cambridge, Mass. (1972).

E. R. Van Driest, *On Turbulent Flow Near a Wall*, J. Aero. Sci. *23*, 1007 (1956).

W. E. Watt, *The Velocity-Temperature Mixing Layer*, University of Toronto, Dept. Mech. Eng. Report TP6705 (1967).

O. Zeman and J. L. Lumley, *Buoyancy Effects in Entraining Turbulent Boundary Layers--A Second-Order Closure Study*, Paper 6C, pp. 6.21-6.27 (1977).

Distribution for ANL-77-78

Internal:

J. A. Kyger
R. Avery
L. Burris
D. W. Cissel
S. A. Davis
B. R. T. Frost
E. V. Krivanec
R. J. Teunis
C. E. Till
R. S. Zeno
H. O. Monson
P. B. Abramson
H. H. Hummel
Kalimullah
P. R. Huebotter
A. R. Brunsvold
Y. S. Cha
B. Chen
J. DePaz
H. M. Domanus
P. A. Howard
K. A. Kasza
P. Kehler
J. L. Krazinski
I. H. Lin
J. J. Lorenz
J. T. Madell
C. C. Miao
J. J. Oras
A. W. Schaeper
R. C. Schmitt
W. T. Sha (35)
V. L. Sha
W. R. Simmons
C. C. Stone
C. I. Yang
G. S. Rosenberg
R. A. Valentin
M. W. Wambsganss
S. S. Chen
Y. W. Shin
W. L. Chen
D. H. Cho
H. K. Fauske
M. Ishii
T. M. Kuzay
R. K. Lo
W. W. Marr
Y. W. Chang
P. R. Betten
L. K. Chang
E. E. Feldman
R. M. Singer
A. B. Krisciunas
ANL Contract File
ANL Libraries (5)
TIS Files (6)

External:

DOE-TIC, for distribution per UC-79e (164)
Manager, Chicago Operations and Regional Office, DOE
Chief, Office of Patent Counsel, DOE-CORO
Director, Reactor Programs Div., DOE-CORO
Director, INEL, DOE-CORO
Director, DOE-RRT (2)
President, Argonne Universities Association
Components Technology Division Review Committee:
- P. F. Cunniff, U. Maryland
- W. E. Kessler, Commonwealth Associates
- C. H. Kruger, Jr., Stanford U.
- N. J. Palladino, Pennsylvania State U.
- N. C. Rasmussen, Massachusetts Inst. Technology
- M. A. Schultz, Pennsylvania State U.
- A. Sesonske, Purdue U.
- H. Thielsch, ITT Grinnell Corp.
- Y. C. L. S. Wu, U. Tennessee Space Inst.